NASA CR-134551

HYDROGEN GAS EMBRITTLEMENT and THE DISC PRESSURE TEST

by E. J. Bachelet and A. R. Troiano

CASE WESTERN RESERVE UNIVERSITY

prepared for

NATIONAL AERONAUTICS AND SPACE ADMINISTRATION
NASA Lewis Research Center

GRANT NGR-36-027-040

November 30, 1973

NASA CR-134551

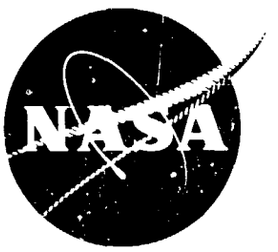

HYDROGEN GAS EMBRITTLEMENT and THE DISC PRESSURE TEST

by E. J. Bachelet and A. R. Troiano

CASE WESTERN RESERVE UNIVERSITY

prepared for

NATIONAL AERONAUTICS AND SPACE ADMINISTRATION
NASA Lewis Research Center

GRANT NGR-36-027-040

November 30, 1973

ACKNOWLEDGEMENTS

This report was submitted by one of the authors, E.J.Bachelet, as partial fulfillment of the requirements for the Degree of Master of Science.

The authors wish to express their gratitude for the unselfish contributions of time and ideas by Professor R. F. Hehemann, Dr. Hugh Gray and J. P. Fidelle.

TABLE OF CONTENTS

Page

ACKNOWLEDGEMENTS i
TABLE OF CONTENTS ii
LIST OF TABLES AND FIGURES iii
SUMMARY vi

INTRODUCTION 1

MATERIALS AND PROCEDURES 10
A. MATERIALS 10
B. PROCEDURES 10
a. DiscPressure Test 10
b. Tensile Tests 15
c. Scanning Electron Microscope 15
d. Permeation Cell 15
e. Gas Environment 15

EXPERIMENTAL RESULTS 17
A. Inconel 718 17
B. L-605 24
C. A-286 25

REVIEW OF THE EMBRITTLEMENT PROCESS 28
A. Adsorption Dissociation 28
B. Absorption Into Solution and Diffusion 30

DISCUSSION 32

SUMMARY OF RESULTS 36

REFERENCES 37

LIST OF TABLES AND FIGURES

Table		Page
I	Composition of the Materials	42
II	Thermo-Mechanical Treatments and Room Temperature Mechanical Properties	43
III	Inconel 718, 35% CW, 180°C, Deuterium gas Permeation Data.	44

Figure		
1	Disc Pressure Cell	45
2	Furnace Assembly and Cell	46
3	Inconel 718, 35% CW, Room Temperature, Helium and Hydrogen Pressure-Deflection Curves	47
4	Inconel 718, 35% CW, Room Temperature, Influence of Loading Rate on Helium Pressure-Deflection Curve	48
5	Inconel 718, 35% CW, Room Temperature, Dynamic Loading, Rupture Pressures versus Loading Rates	49
6	Inconel 718, 35% CW, Room Temperature, Static Fatigue	50
7	Inconel 718, 35% CW, Room Temperature Rupture Pressure vs. Time under Hydrogen	51
8	Inconel 718, 35% CW, Dynamic Loading, Rupture Pressures vs. Temperatures for various Loading Rates	52

LIST OF FIGURES (continued)

		Page
9	Inconel 718, 35% CW, Cycling Procedures	53
10	Results of cycling	54
11	Inconel 718, 35% CW, Room Temperature Rupture Aspects	55
12	Room Temperature, Pressure-Deflection Curves under Helium for all Materials Tested	56
13	Inconel 718, Aged, Room Temperature, Dynamic Loading, Rupture Pressures vs. Loading Rates	57
14	Inconel 718, Aged, Room Temperature, Static Fatigue	58
15	Inconel 718, Aged, Dynamic Loading, Rupture Pressure vs. Temperatures	59
16	Inconel 718, $\frac{pH_2}{pH_e}$ vs. Temperature for Aged and for Cold-Worked Conditions	60
17	Inconel 718, Dynamic Loading, Rupture Pressures vs. Cold Work Reductions	61
18	L - 605, Room Temperature, Dynamic Loading, Rupture Pressures vs. Loading Rates	62
19	L - 605, Room Temperature, Static Figure Data	63
20	L - 605, Dynamic Loading, Rupture Pressures vs. Temperatures	64
21	A - 286, Aged and A - 286 CW 50%, Room Temperature, Dynamic Loading, Rupture Pressures vs. Loading Rates	65

LIST OF FIGURES (continued)

		Page
22	A - 286 Aged, Dynamic Loading, Rupture Pressure vs. Loading Rates	66
23	A - 286 Aged and A - 286 50% CW, Dynamic Loading Rupture Pressures vs. Temperatures	67

SUMMARY

Inconel 718 and alloy L-605 are both susceptible to delayed failure in hydrogen gas at ambient temperatures. In addition, both alloys exhibit slow strain rate and temperature dependent loss of ductility over the temperature range from ambient to 438°C (800°F); but not at the low temperature of -78°C (-105°F). This behavior is characteristic of classical strain aging, reversible type of hydrogen embrittlement.

Minor embrittlement of A-286 was observed only at higher temperatures above ambient. Delayed failure studies under hydrogen pressure suggests that the same inherent temperature dependence indicated for Inconel 718 and L-605 also operates here.

Aging of both Inconel and A-286 resulting in second phase precipitation increased the sensitivity to embrittlement and cold working of Inconel 718 increased the embrittlement slightly.

At this time, these data appear to be consistent with either of two mechanisms:

a) The adsorption of hydrogen which lowers the surface energy allowing crack propagation at lower stresses

b) Adsorbed and absorbed diffusible hydrogen resulting in typical, reversible, strain aging embrittlement.

These authors subscribe to the latter (b) of these two mechanisms.

INTRODUCTION

The influence of hydrogen on the mechanical properties of metals has been well documented in the past fifteen years. Hydrogen induces several phenomena which for purposes of clarity will be restated as recently classified (1) :

1. Hydrogen reaction embrittlement sometimes known as hydrogen attack covers those cases in which hydrogen from any source reacts either with itself or with an alloying element of the matrix to form a new identifiable phase. This happens in copper, silver or gold in which H_2O is formed or in low-alloyed steels which are decarburized to form methane. In the blistering of steel, when the hydrogen content exceeds a certain limit, a molecular hydrogen phase precipitates within the material and irreversible cracking occurs. Also the formation of hydrides in niobium, zirconium, titanium, etc...may be included. Their influence upon mechanical properties is best evidenced in fast strain rate tensile tests or impact tests. They also show up in internal friction studies.

2. Internal hydrogen embrittlement refers to the classical static fatigue and slow strain rate behavior of precharged specimens.

3. Hydrogen environment embrittlement is defined as the embrittlement occurring in a hydrogen gas atmosphere with no formation of a new phase.

The two last phenomena have many common features. So although this study is devoted to the latter, the characteristics of internal reversible hydrogen embrittlement will be reviewed.

Extensive investigations were first made on the very sensitive bcc high strength steels by means of a static fatigue test, well suited for a quantitative study of the phenomenon. These studies involved

specimens that were electrolytically or thermally charged, cadmium plated, and the hydrogen distribution made homogeneous by baking at slightly elevated temperatures. The temperature dependence of the phenomenon, the influence of the hydrogen content, notch geometry and stress level as well as the study of crack propagation suggested an embrittling process paced by the diffusion of hydrogen towards regions of high triaxial stresses where it decreased the lattice cohesive strength (2).

This concept was then extended to titanium alloys (3). The fcc materials initially believed to be immune were later shown to be subject to this strain aging type of embrittlement. A hydrogen induced brittle delayed failure was observed in K Monel, age hardened to obtain a room temperature yield strength of 1.37GN/m^2(185,000 psi) (4). Hydrogenated notched specimens (1.62GN/m^2 NTS) (230,000 psi) statically loaded at 204°C (400°F) yielded time to fail versus applied stress curves exhibiting the same fundamental characteristics already observed in bcc metals:

1. A stress region over which delayed failure occurs by a series of successive crack initiations.
2. A lower critical stress below which failure does not occur.

3. In the case of bcc metals an incubation time for the crack initiation, depending on the hydrogen content. In K Monel, no such incubation time was observed; this could be explained by the high concentrations of hydrogen in the zone where cracking initiated.

In addition it was found that the mechanical properties were recovered after an outgassing treatment.

For delayed failure to occur in bcc as well as in fc materi. three conditions seem necessary:

1. The materials tested must have a yield strength higher than a certain minimum. This has recently been experimentally demonstrated for bcc materials (5) and can be rationalized on the basis that the interaction between hydrogen and a crack embryo or crack tip is due to the stress field. It follows that the interaction energy is limited by the yield strength of the material. Low yield strengths do not allow local build up to the critical hydrog concentrations necessary for cracking (2).

2. The material must be notch sensitive. In the metals which are not notch sensitive a crack is rapidly blunted by plastic deformation and its propagation stops. On the other hand, in notch sensitive materials large amounts of elastic energy can be stored around the crack, which cause it to progress by large steps.

3. A test temperature high enough to provide sufficient hydrogen mobility but not so high as to prevent sufficient concentration by kinetic activity.

Usually these requirements are met at room temperature by bcc materials. They typically have a relatively large hydrogen diffusivity of the order of 10^{-7} cm^2/sec (6), high yield strength and notch sensitivity.

These requirements were also met by K Monel and the titanium alloys in the conditions in which they were tested.

However, to be embrittled, fcc metals require amounts of hydrogen one or two orders of magnitude greater than bcc metals due to their much larger hydrogen solubility. Typically, in a high strength steel, 5 ppm hydrogen will be extremely deleterious to the material, whereas in a fcc materials the amount required is of the order of several hundred ppm. They also rarely satisfy simultaneously the three aforementioned conditions. At the temperatures at which hydrogen has sufficient mobility, the strength levels are very low and there is very little notch sensitivity. This may explain, for instance, why delayed failures of austenitic stainless steels have not yet been observed (7, 8).

Another manifestation of internal hydrogen embrittlement is evidenced by slow strain rate tensile tests of hydrogenated specimens. Most metals are sensitive to this phenomenon. Even non-transition alloy type aluminum (9) was recently found to possess the following characteristic features:

1. Hydrogen has no significant effect on the elastic properties of bcc materials. Their elastic modulus is unchanged. It can produce a small yield point in pure iron at low temperatures. At room temperature it can prevent the occurrence of the yield point phenomenon usually found in mild steel.

In fcc metals, the elastic modulus is unchanged. The flow stress (.2%) is slightly affected. At liquid helium temperatures this effect, which is of the order of 10%, is at its maximum. It decreases as temperature increases to become negligible at about 227°C (440°F). In pure nickel a Portevin-Le Chatelier effect has been found around -80°C (-112°F) (10).

2. The room temperature work hardening rate is not significantly altered by the addition of hydrogen.

3. The ductility parameters are reduced in proportion to the hydrogen content.

4. Low strain rates enhance the embrittlement.

5. The effect is maximum near room temperature.

6. The fracture type is changed from that of a typically ductile metal to that of a typically brittle metal.

7. The phenomenon is reversible with respect to outgassing.

The concepts drawn from the static fatigue experiments could be extended with reasonable success to the above behavior. For bcc metals the extension was straight-forward. The deformation creates the high triaxial stress zones and the mechanism previously described starts to operate. The incubation period is merely hidden by the continuous nature of the deformation (2). In fcc metals it was assumed that the plastic deformation created dislocation pile-ups. The elastic stress field associated with them induces the diffusion and accumulation of hydrogen in the pile-up region, decreasing their strain energy and causing the leading dislocations to coalesce, thus creating a crack

embryo. The slight pinning of the nearby dislocation sources as evidenced in the flow stress behavior tended to make plastic relaxation more difficult and therefore such a crack embryo more effective as a stress raiser. The temperature and strain rate dependence could be derived from the competition between the relaxation of the pile-ups and the diffusion of hydrogen. It was also suggested that the diffusion of hydrogen to the dislocation pile-ups might be influenced by processes which occur during the plastic flow. Particularly significant in this respect was the fact that at -196°C (-321°F) there was no loss of ductility at high strain rates but some at smaller strain rates (4).

All these studies had been initiated by problems encountered in industry. Hydrogen can be picked up by such processing operations as electroplating, melting or pickling. Relatively recently, the aerospace industry has been plagued with a new hydrogen embrittlement problem; advanced rockets and gas turbine engines are planned to operate in environments containing hydrogen gas. Although this type of embrittlement has been known for a few years it is not yet well understood. It shows up in all mechanical properties; tensile and fracture mechanic tests, low and high cycle fatigue, and creep. Again bcc and fcc metals have very different susceptibilities. At room temperature, a few hundred torrs of hydrogen can reduce the threshold stress intensity factor

of 4130 steel by 50% (11,12). Also, some of the nickel base alloys which are among the most susceptible fcc alloys exhibit increased fatigue crack growth rates at only a few hundred torr of hydrogen (13, 14).

Hydrogen environment embrittlement has many features in common with internal hydrogen environment. The ductility parameters are mainly affected. The embrittlement is enhanced by slow strain rates. At low strain rates it is a maximum near room temperature. In a maraging steel exposed to hydrogen gas an incubation period and a discontinuous acoustic emission associated with the cracking process has been found (15).

However, several alloys, particularly nickel base alloys, have been reported to present different susceptibilities to internal and environment hydrogen embrittlement (16). Also it has been said that internal embrittlement cracking initiates inside the specimen whereas environment hydrogen embrittlement initiates at the surface (16).

It should be noted that the fcc nickel base alloys have been compared under different severe testing conditions. The internal hydrogen embrittlement data usually referred to, correspond to the room temperature static fatigue of unnotched specimens loaded at 80% of their yield strength and cathodically polarized (17). No failure occurred within a period of 200 hours. The environment embrittlement data come from test conditions involving plastic deformation in high pressure

hydrogen gas (13, 14). More recently, slow strain rate tensile tests of unnotched Inconel 718 specimens cathodically polarized have yielded a loss in reduction in area of 12% (18). Unfortunately, since the investigators do not specify their heat treatment, comparisons are difficult. However, a 12% loss of unnotched reduction in area was also observed when Inconel 718 was tested in 17 MN/m^2 (2500 psi) hydrogen gas in the annealed condition (19). As pressure increased, the relative reduction in area for hydrogen and helium decreased sharply; at 70MN/m^2 (10,000 psi), the ratio was 0.05(19). More experiments in internal hydrogen embrittlement are needed to have a good comparison.

These observations have led to some controversy about the embrittling mechanism. Is it merely a new form of internal hydrogen environment with three additional steps required in the embrittling process? These would be adsorption, dissociation, and absorption. Or is it a truly new phenomenon? Two surface dependent mechanisms have been proposed (16). One is based on the heat of absorption of hydrogen which decreases the strain energy to initiate a crack. The second mechanism is the absorption of hydrogen into the surface where it lowers the surface ductility, possible by inhibition of dislocation generation at the surface or by increasing the lattice friction stress for dislocation motion at the surface.

The present study is directed towards three high temperature superalloy candidates for aerospace applications: nickel base Inconel 718, cobalt base L-605 and iron base A-286. All three have an austenitic structure, can be precipitation hardened and are alloys of transition metals.

Previous investigators show Inconel 718 to be severely embrittled by high pressure gaseous hydrogen. In slow strain rate room temperature tests, large reductions of ductility, notch strength, threshold stress intensity, and low and high cycle fatigue are observed (13,14,19, 20,21,22). The embrittlement was found to vary with heat treatment (20).

The threshold stress intensity of A-286 was not affected in 35 MN/m^2 (5,000 psi) hydrogen at room temperature (20). After a very severe thermal charging (24 hours at 400°C (750°F) under 31 MN/m^2 (4,500 psi), slow strain rate tests at 0°C (32°F) have shown a loss of reduction in area of 45.5% (23). No data on the embrittlement of L-605 was available to us.

The main feature of this investigation is its original test technique, the disc pressure test described in the next section.

MATERIALS AND PROCEDURES

A. MATERIALS

The compositions of Inconel 718, L-605 and A-286 used in this study are listed in Table I. All materials were received in the form of 0.64 mm (0.025 in.) thick sheets, annealed and cold worked. Inconel 718 and A-286 were annealed and aged in order to study the influence of a second phase on the embrittlement. The materials and thermomechanical treatments tested are as follows:

a) Inconel 718

- Mill annealed one hour at 980°C (1800°F)
- Mill annealed and 20% cold worked
- Mill annealed and 35% cold worked
- Annealed one hour at 940°C (1725°F), aged eight hours at 720°C (1325°F), furnace cooled to 620°C (1150°F) and held at that temperature for eight hours.

b) L-605

- Annealed one hour at 1230°C (2250°F) and 45% cold worked.

c) A-286

- Annealed one hour at 980°C (1800°F) and cold worked 50%.
- Annealed one hour at 980°C (1800°F) and aged 16 hours at 720°C (1325°F).

B. PROCEDURES

a) The disc pressure test

The test consists of applying pressures of either hydrogen or helium on the lower side of a circular disc. Figure 1 represents a schematic drawing of the cell and Figure 2 is a photograph of the cell and furnace assembly for medium temperature testing.

Under an increasing gas pressure, the disc undergoes first elastic, then plastic deformation until rupture. This will be referred to as a dynamic test. If the gas pressure is held constant at a pressure less than the rupture pressure, one has a static fatigue test which can lead to delayed catastrophic failure with hydrogen gas.

To describe the mechanical state of the disc at a given time two quantities are measured: the gas pressure and the deflection of the disc at its center. The pressure versus deformation curves were automatically recorded for all materials in the following way. Deflections were measured by means of a differential transformer transducer SATEC type 9234. It is linear variable displacement type for use with a type 6101-E demodulator. Its linearity is $\pm$ 1% with a stroke to 6.35mm (0.250 in.) . It was checked and calibrated with a precision micrometer before use.

Pressures were measured by means of a carbon resistor

pressure potentiometer operative in the range of pressures up to 31 MN/m^2 (4,500 psi). It was calibrated on a precision manometer. Pressures higher than 31 MN/m^2 (4,500 psi) could not be automatically recorded. They were directly read on the manometer.

The strains in the disc are not uniform and a strain rate cannot be defined for the much the same reasons as in any notch test. Instead a loading rate is defined as the pressure increase per unit of time. This was chosen on the basis that the deformation characteristics of unhydrogenated fcc metals do not depend very much upon the strain rate. On the other hand, for a metal deformed in a hydrogen environment the most important variable is the rate of availability of hydrogen given by the pressure increase per unit of time.

Rupture generally occurs at the edge of the disc where it is clamped and where the plastic deformation is maximum. For fcc metals, it is that highly localized plastic deformation which makes the test procedure a very sensitive one, as will be seen later.

A parameter had to be chosen to measure the degree of embrittlement. Rupture pressures in helium and in hydrogen gas are useful for engineering applications. However, they are complex functions of both the strength and the ductility of the materials. The room temperature deflection measurements are representative of the ductility of

the materials and they were taken to represent the degrees of embrittlement.

As in notch tests, interpretation of the results requires care. The following discussion is aimed at aiding in an understanding of the test. All experiments performed thus far on a large variety of materials show that within the limit of accuracy of the measurements, the deformation versus pressure curves of a material with hydrogen or helium gas are the same except for the total amount of ductility, see Figure 3. Thus it follows that for a given temperature and loading rate a gas can act upon the system in two different ways, as a loading factor and as an environmental factor.

- Loading factor: A given pressure, whatever the gas may be, determines the same macroscopic state of stress which is dependent only on the mechanical properties of each material.

- Environmental factor: hydrogen may also be considered as an environmental factor. It has a chemical potential which makes it able to interact with the surface, permeate through the material, interact with defects and embrittle the material.

It is the similarity between the deformation versus pressure curves for both gases which enables one to separate these two actions of the gases. In this respect, the test is unique.

It can now be seen that in an unnotched or notched tensile test

or in a fracture mechanics test in an atmosphere of hydrogen, the stress state and the chemical potential of the gas are two variables which can be studied independently. Indeed it is important in a study of environmental embrittlement to check the influence of both separately. In the case of the disc test, stress state and chemical potential of the gas are not independent variables. However, it is simple to study them separately by using partial pressures of hydrogen in helium gas or by modifying the cell in order to be able to apply a back pressure of helium on the upper side of the disc.

Another problem arises in the comparison of two different materials or even the same material at two different temperatures. A given deflection generally gives two different states of stress depending upon the elastic constants and hardening characteristics of each material, and generally it corresponds to two different pressures. On the other hand, for different materials or test temperatures, a given pressure generally leads to two different deflections, two different shapes for the strained discs and therefore two different states of stress. It can be

seen that two materials with different mechanical characteristics will generally not be in the same state of stress. It is a common characteristic of all tests such as notch tests or fracture mechanics tests involving an inhomogeneous plastic deformation that the stress state is ill defined. Again applying a back pressure of an inert gas would delay the onset of plastic flow and allow one to study the influence of higher pressures upon elastically strained materials.

The test procedure is fast, simple and inexpensive. As will be seen later, it can yield interesting information about the mechanism of the embrittlement process and it reproduces well the conditions met in some engineering situations (24).

b) Tensile Tests

Tensile tests have been performed in order to provide basic information on the materials. Tensile samples were cut from the 0.64 mm (.025 in.) thick sheets in both longitudinal and transverse directions. Crosshead speed of the Instron testing machine was 1 cm/min (0.39 in./min).

c) Scanning Electron Microscopy

The cracked surfaces were analyzed by means of a scanning electron microscope.

d) Permeation Cell

The permeation of deuterium gas through the Inconel 718 discs was measured in collaboration with the French AEC by a procedure described in (25). A pressure of .07 MN/m^2 (10 psi) is applied under the disc and the flow of hydrogen permeating through the disc is measured as a function of time.

e) Gas Environment

A 99.94% pure hydrogen gas supplied by the Burdett Oxygen Company was used throughout this investigation. The gas pipes and the cell chamber were evaluated and flushed three times with either helium or hydrogen before a test.

EXPERIMENTAL RESULTS

A. INCONEL 718

a). Mill annealed and 35% cold worked

A basic investigation of the test at room temperature was first undertaken on the annealed, 35% cold worked condition. The two measured parameters were the gas pressure and the deflection at the center of the disc. Figure 3 shows the pressure versus deflection curves under helium and hydrogen for a given loading rate. The unusual shape of the curve is due to geometrical and mechanical factors. Stresses and strains are not uniform in the disc. It is not a strain which is plotted but the deflection at the center of the disc which is only indirectly related to the non-uniform strains in the specimen. In helium very little influence of the loading rate on the pressure deflection curve was observed as shown in Figure 4.

Within the limit of accuracy of our measurements, the only effect of the replacement of helium by hydrogen is a reduction of the total ductility in an amount depending on the loading rate. It could be varied from 0.17 MN/m^2 min (25 psi/min) up to 103 MN/m^2 min (15000 psi/min) and its influence is further illustrated in Figure 5. It can be observed that:

- The embrittlement is enhanced by slow loading rates.

- There is a reproducible pressure below which the discs do not fail. That lower rupture pressure of 21 MN/m^2 (3000 psi) is well above the onset of plastic flow which occurs at about 2 MN/m^2 (300 psi), See Figure 3.

At this point, the influence of surface conditions was tested. No difference in the lower pressure was found for either as-received or sanded (600 paper) discs.

Static fatigue tests were then performed at room temperature. Two procedures were used:

1) Straining with hydrogen and exposure a given pressure.

2) Prestraining with helium, unloading an loading with hydrogen to that pressure.

A high loading rate of 103 MN/m^2 min (15000 psi min) was chosen in order to minimize the loading time and loading rate influence on the results. This type of experiment led to some scatter in the results. The pressures versus times to fail are plotted in Figure 6 for both procedures, which do not exhibit significantly different results considering the scatter. The longest time of exposure was 3 weeks at 34 MN/m^2 (5000 psi). For the discs directly deformed in hydrogen gas, the times to fail were shorter and failures could be obtained for slightly lower pressures than in the case of the discs prestrained in helium. This indicates a slight influence of the deformation in hydrogen even

though the loading rate was high. On the same Figure 6, the rupture pressures versus total times of exposure to hydrogen gas in dynamic experiments are also plotted. For example, if a dynamic test conducted at a loading rate of 1.7 MN/m^2 min (250 psi/min) led to a rupture pressure of 27 MN/m^2 (3900 psi) as indicated in Figure 5, then, on the dotted line in Figure 6, 27 MN/m^2 is plotted versus $\frac{2.7 \quad MN/m^2}{1.7 \quad MN/m^2 \, min}$ which equals 16 minutes. A comparison of the three curves in Figure 6 shows that at room temperature, dynamic experiments at slow strain rates represent more severely embrittling situations than static fatigue experiments. Failures occur at much lower pressures and in shorter times. All these results indicate a significant influence of the straining in hydrogen and of the loading rates on the embrittlement.

The influence of static fatigue at an intermediate pressure was checked. Discs were strained under hydrogen gas at a loading rate of 10 MN/m^2 min (1500 psi min) up to 21 MN/m^2 (3000 psi) and held at that pressure for various times. Then they were unloaded and strained to rupture under helium at a loading rate of 10 MN/m^2 (1500 psi/min). Figure 7 shows rupture pressure versus time of exposure at 21 MN/m^2 (3000 psi). There is a slight but significant decrease in the rupture pressures. During the holding time at 21 MN/m^2 (3000 psi) hydrogen slowly deteriorates the materials.

At this point, attempts were made to detect discontinuous crack propagation and incubation times in static fatigue tests. Two types of equipment were used: a tape recorder with a sensitive microphone located next to the disc, and a strain indicator recording strain variations in a strain gage attached to the disc. No conclusive indications were obtained. Crack propagation in fcc materials releases little energy and the equipment was not sensitive enough. In the same type of experiment, a maraging steel disc exposed to 7 MN/m^2 (1000 psi) H_2 gas emits a very audible discontinuous accoustic emission associated with cracking (15).

Another variable examined was test temperature. It was varied from -79°C (-105°F) to 438°C (800°F) and several loading rates were used to strain the discs. The results of dynamic tests are plotted in Figure 8. Four observations can be made:

1. The dynamic embrittlement is most severe near room temperature.

2. The influence of the loading rate is a maximum near room temperature. It is still apparent at 93° C (200° F) and becomes less important as the temperature is raised.

3. At 93°C (200°F), to get the same degree of embrittlement as at room temperature, slower loading rates are needed. For example, for a loading rate of 10 MN/m^2 min (1500 psi/min),

there is a noticeable embrittlement at room temperature whereas at 93°C (200°F) it is almost zero. For the same loading rate at 204°C (400°F) the embrittlement reappears.

4. At the lowest temperature examined, -76°C (-105°F) and for the strain rate used, no embrittlement appears.

The influence of static fatigue was not systematically studied at the higher temperatures. However, a few data points at 93°C (200°F) show that at that temperature, just as at room temperature, a dynamic experiment at a slow loading rate constitutes a more severely embrittling situation than a static fatigue test. A disc was exposed under a pressure of 39.6 MN/m^2 (5750 psi), with a loading rate of 10 MN/m^2 min (1500 psi/min), for 24 hours without failure. The pressure was then slowly raised up to 41.4 MN/m^2 (6000 psi). At that point the disc broke. With the same loading rate, another disc was exposed at 132°C (270°F) under a pressure of 35 MN/m^2 (5000 psi) for 48 hours without failure.

The influence of pressure cycling was studied. At room temperature, 20 pressure cycles over a period of 24 hours at the following pressures: 1.4 MN/m^2 (200 psi), 3.5 MN/m^2 (500 psi), 7 MN/m^2 (1000 psi) and 14 MN/m^2 (2000 psi), followed by a slow dynamic straining led to no decrease in the lower rupture pressure.

Figure 9 describes additional procedures involving pressure and temperature cycles. Figure 10 indicates that they had no influence on the embrittlement characteristics. All cycling was manually performed; a more systematic study of low cycle fatigue would require automation of the cycling of the pressure.

The permeation characteristics have been measured as previously described. The flow of deuterium at 180°C (356°F) under an upstream pressure of 1 MN/m^2 (145 psi) was recorded as a function of time. The establishment of steady state permeation under those conditions required 125 hours. Assuming that the permeation process is not surface controlled, analysis of the pressure versus time curve after correction to one atmosphere yields the permeability, diffusivity and solubility parameters listed in Table III. Extrapolation of these data to room temperature yields a value of 2.4×10^{-11} $cm^2/sec.$ A literature review of the isotopic effects on diffusion shows that the ratio $\frac{D\ hydrogen}{D\ deuterium}$ always equals $1.24 \pm .3$. This yields a value of D hydrogen at room temperature of the order of 3×10^{-11} $cm^2/sec.$ Such an extrapolation is only indicative. However, it suggests a very slow diffusion process.

Finally, the room temperature fracture was examined. Figure 11

shows the fracture aspects after rupture due to either hydrogen or helium gas. In the case of helium ductile rupture is observed. The hydrogen induced rupture occurs along the rolling direction. It is brittle and mainly intergranular with a few evidences of transgranular cracking.

b). The aged condition

The alloy was then aged in order to study the influence of second phase precipitation on the embrittlement characteristics Figure 12 shows the corresponding pressure deflection curve. At room temperature, the rupture pressures under helium and hydrogen gas versus loading rates are plotted in Figure 13. Again decreasing the loading rate enhances the embrittlement. The resistance of the material to helium pressure was the same as the 35% cold worked condition. But the lower critical pressure in hydrogen was reduced to 14 MN/m^2 (2000 psi). The aging treatment seems to increase the embrittlement.

Static fatigue data are plotted in Figure 14. The material was prestrained under helium, unloaded and then reloaded with hydrogen. It can be noted that the lower rupture pressure 31 MN/m^2 (4500 psi) obtained in these conditions is lower than that found for the 35% cold

worked alloy. The ratio $\frac{pH_2}{pHe}$ decreases from .75 to .55.

The temperature dependence of the embrittlement for the slow loading rate of .35 MN/m^2 min (50 psi/min) is illustrated in Figure 15. The behavior is qualitatively the same as previously found with the only exception that no minimum in the embrittlement is observed at 95°C (200°F) as in the 35% cold worked alloy. In Figure 16 the ratio $\frac{pH_2}{pHe}$ obtained with the lowest loading rates are plotted as a function of temperature for both the cold worked and the aged condition. The ratios are the same at 438°C (800°F). Below that temperature the aging treatment markedly influences the embrittlement.

c. The annealed condition and the annealed and 20% cold worked condition.

The pressure deflection curves of Inconel 718 discs with the same thickness but in these new conditions are plotted in Figure 12. In Figure 17, the lower rupture pressures observed under hydrogen gas and the corresponding helium rupture pressures are plotted for all conditions tested. Over the range of cold work studied (0 - 35%) the degree of embrittlement increases slightly with the amount of cold work.

B. L - 605

The pressure deflection curve of this alloy is plotted in Figure 12. Tests were first conducted at room temperature. Figure 18 shows that as in Inconel 718, slow loading rates enhance the embrittlement.

Static fatigue data of Figure 19 present the times to fail after a prestrain under helium at a given pressure followed by a reloading with hydrogen to the same pressure. The rupture pressures versus total times of exposure to hydrogen gas in dynamic experiments are also plotted, the same as was done for Inconel 718 in Figures 6 and 14. The behavior of L-605 is now different from that observed for Inconel 718. Failure occurs sooner when the discs are held at pressure than when they are slowly and continuously loaded up to that pressure. This is discussed later. Attempts to detect a discontinuous crack propagation and incubation times were unsuccessful for much the same reasons as in Inconel 718.

The temperature dependence of the embrittlement is presented in Figure 20. Several loading rates were used. Qualitatively, the results are the same as in the case of Inconel 718 aged. Static fatigue experiments at 93°C (200°F) yield the same results as at room temperature. Static fatigue leads to embrittlement sooner than slow

dynamic testing.

C. A - 286

This alloy was tested in two different conditions

- Annealed and aged

- Annealed and cold worked 50%

The corresponding pressure deflection curves are shown in Figure 12.

At room temperature, for neither condition was a reduction in the rupture pressure observed after substitution of hydrogen for helium, see Figure 21. The slowest loading rate used was .35 MN/m^2min (50 psi/min).

For the same slow loading rate, the influence of temperature on the rupture pressures of the aged material is plotted in Figure 22. The embrittlement increases with temperature up to 204°C (400°F), then decreases slightly up to 438°C (800°F).

Holding a disc for 48 hours under 8.6 MN/m^2 (1250 psi) hydrogen pressure at 93°C (200°F) and loading it to rupture at .35 MN/m^2 min (50 psi/min) decreased the rupture pressure from 41.8 MN/m^2 (6050 psi) to 37.4 MN/m^2 (5350 psi). The same experiment at 438°C (800°F) decreased both helium and hydrogen rupture pressures

without however altering the ratio $\frac{pH_2}{pHe}$. This may be due to overaging or creep.

For A-286, as for Inconel 718, a slow dynamic test is more severely embrittling than a static fatigue test. A disc was exposed at 204°C (400°F) under 38 MN/m^2 (5500 psi) hydrogen after prestrain under helium. It did not fail within 100 hours.

The temperature dependence of both helium and hydrogen rupture pressures for A-286 annealed and cold worked 50% is illustrated in Figure 23. As the temperature was raised the rupture pressure in helium of this severely cold worked alloy decreased. At the highest temperature tested some embrittlement appeared.

REVIEW OF THE EMBRITTLEMENT PROCESS

Before discussing the results of this investigation the possible steps occurring in the embrittlement process will be examined. Data in the literature will be reviewed and discussed.

A. The Adsorption, Dissociation Step.

The initial step in any hydrogen environment embrittlement mechanism involves the interaction of the gas with the metal surface. At room temperature, the range in which the embrittlement is at its maximum, most metals are covered with oxides which have to be penetrated or ruptured in order for the gas to reach the metal. The reactions of hydrogen with the clean metal surface itself are extremely complex. These surfaces are extremely heterogeneous. In addition adsorption and displacement phenomena caused by foreign gases can play an important role especially when oxygen is involved. For example, on the 111 plane of tungsten, preadsorption of oxygen blocks the subsequent adsorption of hydrogen on some sites at both -148°C (-235°F) and 27°C (80°F). At 27°C (80°F)preadsorbed oxygen at an exposure as small as 5×10^{-5} torr second can completely inhibit subsequent hydrogen adsorption. On W(211) at 27°C (80°F) the same behavior is observed. The saturation amount of hydrogen adsorbed falls linearly

with oxygen precoverage to reach zero when the oxygen precoverage is complete. The reverse situation has been investigated. When hydrogen is preadsorbed and the surface then exposed to various amounts of oxygen, it is found that on W [111] at 27°C (80°F) at low pressure exposures, oxygen fills "in the gaps" in the adsorbed hydrogen.

At higher oxygen exposures, the displacement of hydrogen by oxygen occurs. At an oxygen exposure of 4.7×10^{-5} torr second, the hydrogen coverage remaining was only 0.047 of the surface. Although the surfaces of the 3 superalloys tested in this investigation are more complex than a plane of pure tungsten, the relative behaviors of oxygen and hydrogen are probably similar to what is reviewed above (26,27). Oxygen impurities are probably one of the main reasons for the lack of reproducibility of hydrogen embrittlement data among various investigators.

It should be noted that the surface sites more likely to play a role are high energy surface sites associated with defects in the crystal structure, such as grain boundaries, slip steps, or dislocation ends. The importance of this chemisorption dissociation step in hydrogen environment embrittlement has been shown numerous times. When atomic hydrogen is provided near the crack tip by a heated tungsten

filament, crack growth rates are several orders of magnitude greater than rates in molecular hydrogen; crack growth persists when the temperature is raised up to 164°C (328°F) whereas it decreases in molecular hydrogen (12). These test results confirmed that in this material, hydrogen adsorption and dissociation is a transfer step which is the overall rate controlling step in the process of hydrogen environment embrittlement. In another experiment with 4130 steel, the dependence of crack growth rate upon temperature suggests that the controlling step of the process is adsorption dissociation (11). It should be noted that both experiments were performed in high strength bcc steels in which the hydrogen diffusivity is relatively high. Finally, embrittlement is inhibited by oxygen concentrations as low as 200 ppm (28, 29).

B. Absorption into Solution and Diffusion

Hydrogen can diffuse through the metal in several ways:

a) Intergranular diffusion

b) Transgranular lattice diffusion under the influence of a concentration or a stress gradient. In the internal reversible embrittlement of bcc metals, diffusion due to the stress gradient caused by an artificial notch was found to be the rate controlling step for the embrittlement phenomenon (2). More recently in a high strength bcc steel penetration of hydrogen gas

during straining could be rationalized by lattice diffusion (30).

c) Strain enhanced diffusion can possibly play a role as proposed a long time ago to explain the strain rate effect (31). There are indeed numerous examples of an interaction of hydrogen with dislocations. The internal friction peak found in 310 stainless steel (32) was explained by this interaction. Since then such a peak has been found in very different metals such as nickel, copper, etc...(33). A serrated stress strain curve was observed in nickel monocrystals cathodically polarized during deformation (34). At the potential used, 600 mV (SCE) hydrogen was produced on the surface of the specimen. Serrations were observed even though calculations indicated that the depth of penetration of hydrogen could not be greater than 15 microns. Serrations were considered as experimental evidence for the existence of surface or near surface dislocation sources. The role of plastic straining in enhancing the diffusion of hydrogen may become especially important for metals with a low diffusion coefficient for hydrogen.

DISCUSSION

In the case of Inconel 718, in all conditions tested, the most important characteristic is the difference between static fatigue and slow loading rate dynamic experiments as shown in Figure 5 and Figure 14.

There may be several explanations for this behavior:

1. The gas purity may be responsible. It is possible that in a static fatigue experiment, impurities such as oxygen molecules, preferentially adsorbed on the freshly created metal surfaces inhibit hydrogen adsorption and therefore any embrittlement mechanism. One would have to assume that in a slow dynamic test such a process is not effective.

2. Another explanation might be provided by the plastic relaxation of crack embryos in static fatigue tests, before hydrogen is present in an amount sufficient to react with them.

3. This behavior is also compatible with an internal embrittlement mechanism in which processes occurring during plastic deformation greatly enhance the absorption and diffusion processes as suggested in the preceeding section. In static fatigue tests, the times involved in the embrittling process might be so long that no failure is observed. At room temperature, 21 days under 35 MN/m^2 (5000 psi) H_2, was the longest static fatigue test performed in the 35% cold worked condition. This is a short time in view of the slow diffusion.

4. An embrittlement mechanism based only on the lowering of the surface ductility by pinning of surface dislocation sources, or increase in the lattice friction stress cannot explain the embrittlement observed when the material is prestrained under helium and then reloaded at the same pressure under hydrogen. The ratio $\frac{pH_2}{pHe}$ in this case falls

down as low as .5 in the aged condition. However, contributions from such a process may explain the greater embrittlement observed at room temperature in slow dynamic experiments. Reducing the surface ductility will enhance the tendency to brittle failure.

The next step in this study involves analysis of the hydrogen content of the specimens in the various testing conditions which should provide information leading to a better understanding of the process.

In the case of the cobalt base alloy, L-605, again an embrittling mechanism based on the reduction of the surface ductility of the material must be disregarded. It cannot explain the static fatigue data presented in Figure 19.

The behavior observed for L-605 is different from that of inconel 718, at room temperature and at 93°C (200°F). Prestraining in helium at a given pressure leads to failure sooner than slow rate dynamic testing in hydrogen. [illegible] is consistent with either an internal embrittlement mechanism or with a mechanism in which the surface energy of the metal is lowered by hydrogen adsorption. Because times to fail observed in static experiments are so short (approximately 30 minutes) an internal mechanism would require fast hydrogen absorption and possibly diffusion. The amounts of hydrogen required to embrittle the material may also be smaller than

in the case of Inconel 718. A knowledge of $D_{hydrogen}$ in this alloy would be useful. Again, hydrogen analysis of the specimens after failure might be conclusive.

A-286 displayed no evidence of embrittlement at room temperature in the two conditions tested. It is not however an intrinsic property of its matrix. Dynamic experiments on the aged material between 204°C (400°F) and 438°C (800°F) yield ratios $\frac{pH_2}{pHe} = 0.8$ very similar to those obtained with Inconel 718 and L-605 in this temperature range.

The absence of embrittlement of A-286 at room temperature may be related to:

1. The very low diffusion coefficient at room temperature as measured by (25).

2. The inherent high fracture toughness of this alloy

The fact that 48 hours exposure at 93°C (200°F) under 8.6 MN/m^2 (1250 psi) hydrogen slightly lowered the rupture pressure suggests that diffusion plays a role in the embrittlement process and that the temperature dependence of the embrittlement is intrinsically the same as that of Inconel 718 and L-605. Near room temperature one step in the embrittling process may be very slow and mask embrittlement during the relatively short dynamic tests. Critical experiments would involve

cycling the temperature between room and higher temperatures.

Again a hydrogen analysis of the samples might provide conclusive evidence about the embrittling mechanism.

SUMMARY OF RESULTS

1. Inconel 718 and L-605 are susceptible to delayed failure in a gaseous hydrogen environment at room temperature.

2. Inconel 718 and L-605 are subject to slow strain rate embrittlement between room temperature and 438°C (800°F).

3. The strain rate and temperature dependence of these phenomena in this temperature range is the same as observed in internal reversible embrittlement.

4. For Inconel 718 and L-605 no embrittlement is observed at a low temperature of -78°C (-105°F).

5. No embrittlement is observed at room temperature for A-286.

6. For A-286 some embrittlement appears at higher temperatures. Holding in hydrogen for periods of time suggests the same intrinsic temperature dependence as Inconel 718 and L-605.

7. An aging treatment leading to second phase precipitation in Inconel 718 and A-286 enhances the embrittlement.

8. For Inconel 718, the embrittlement increases slightly from a 0% cold work reduction to a 35% cold work reduction.

9. An embrittling mechanism based on the reduction of the surface ductility must be disregarded. It can however increase the tendency to brittle failure in slow strain rate experiments for Inconel 718.

10. Two mechanisms are consistent with our data:
    a) Hydrogen adsorption lowers the surface energy causing crack propagation at lower stresses.
    b) The concepts proposed to explain internal embrittlement may be successfully applied to hydrogen environment embrittlement.

11. The disc pressure test has proven itself to be a valuable tool in the study of hydrogen environment embrittlement.

REFERENCES

1. Hugh Gray, "Testing for Hydrogen Environment Embrittlement: Experimental Variables", in Hydrogen Embrittlement Testing, ASTM STP-543, pp.133-151, 1974.

2. A. R. Troiano, "The Role of Hydrogen and Other Interstitials in the Mechanical Behavior of Metals", Edward DeMille Campbell Memorial Lecture, Trans,ASM, Vol.52, pg.54, 1960.

3. R. D. Daniels, R.J. Quigg and A.R.Troiano, "Hydrogen Embrittlement and Delayed Failure in Titanium Alloys". Trans. ASM, Vol. 51, pg. 843, 1959.

4. J. L. Mihelic, A.R.Troiano, "Solute Induced Embrittlement in Steel and Several Face-Centered Cubic Alloys", ARL 64-101, June 1964.

5. M. F. McGuire, R.F.Hehemann and A.R.Troiano, "Stress Corrosion Cracking and Hydrogen Embrittlement in 410 Stainless Steel". International Congress, Hydrogen in Metals, Paris, Vol. 2, pg. 325, 1972.

6. H.L.Eschlack, F.Gross and S.Schulien, "Permeability Measurements with Gaseous Hydrogen for Various Steels". Vacuum, Vol. 13, pg. 543, 1963.

7. J. Papp, Master Thesis,"Stress Corrosion Cracking in 310 Austenitic Stainless Steel",CWRU, 1973.

8. J.P.Fidelle, "Hydrogen Embrittlement and Stress Corrosion Cracking of Austenitic Stainless Steels in Chloride Media", French AEC Report, R-4361, October 1972.

9. R. N. Gest and A.R.Troiano,"Hydrogen Embrittlement and Stress Corrosion Cracking in Aluminum Alloys". International Congress, Hydrogen in Metals, Paris, Vol.2, pg. 427, 1972.

10. T. Boniszewski and G.C.Smith, "The Influence of Hydrogen on the Plastic Deformation, Ductility and Fracture of Nickel", Acta.Met., Vol. 11, pg. 165, 1963.

11. D.P.Williams and H.G.Nelson, "Embrittlement of 4340 Steel by Low-Pressure Gaseous Hydrogen", Metallurgical Transactions, Vol.1, No. 1, pp.63-68, January, 1970.

12. H.G.Nelson, D.P.Williams and A.S.Tetelman, "Embrittlement of a Ferrous Alloy in a Partially Dissociated Hydrogen Environment", Metallurgical Transactions, Vol.2, No.4, pp.953-959, April 1971.

13. R.J.Walter, and W.T.Chandler, "Influence of Hydrogen Pressure and Notch Severity on Hydrogen Embrittlement", Materials Science and Engineering, Vol.8, pp.90-97, 1971.

14. J.A.Harris, Jr. and M.C. VanWanderhan, "Properties of Materials in High Pressure Hydrogen at Cryogenic, Room and Elevated Temperatures", Technical Report PWA-FR-4566, NASA CR-119884, Pratt and Whitney Aircraft, West Palm Beach, Florida, June 1971.

15. J.P.Fidelle and A.R.Troiano, "Hydrogen Embrittlement and Stress Corrosion Cracking". International Congress, Hydrogen in Metals, Paris, Vol. 1, pg. 31, 1972.

16. R. J. Walter, R. P. Jewett and W. T. Chandler, "On the Mechanism of Hydrogen Embrittlement of Iron and Nickel Base Alloys", Materials Science and Engineering, Vol.5, pp.98-110, 1970

17. T.P.Groeneveld, E.E.Fletcher and A.R.Elsea, "A Study of Hydrogen Embrittlement of Various Alloys", Technical Report NASA CR-77374, Battelle Memorial Institute, Columbus, Ohio, June 1966.

18. D.L.Dull and L.Raymond, "Surface Cracking of Inconel 718 During Cathodic Charging", Met. Trans., Vol.4, No.6, pg.1635, 1973.

19. R.P.Jewett, R.J.Walter, W.T.Chandler and R.P.Frohmberg, "Hydrogen Environment Embrittlement of Metals", NASA, CR-2163, Rocketdyne, Canoga Park, California, March 1973.

20. R.J.Walter, H.G.Hayes and W.T.Chandler, "Influence of Gaseous Hydrogen on Metals", Technical Report R-8716, NASA, CR-119917, Rocketdyne, Canoga Park, California, May 1971.

21. P.M.Lorentz, "Effect of Pressurized Hydrogen upon Inconel 718 and 2219 Aluminum , Technical Report D2-114417-1, NASA CR-100208, Boeing Company, Seattle, Wash., February 1969.

22. V. Frick, G.R.Janser and J.A.Brown, in Space Shuttle Materials, Vol.3, Society of Aerospace Materials and Process Engineers, Azusa, Cal., pp. 597-634, 1971.

23. J.P.Fidelle, "Hydrogen Embrittlement of a Stable Austenitic Steel", French AEC Report, Bruyeres-le-Chatel, 1971.

24. J.P.Fidelle, "Quick Pressure Hydrogen Embrittlement Test of Metal Discs", Colloquium Hydrogen in Metals, Valduc, edited by Le Centre d'Etudes de Bruyeres-le-Chatel, 91, France, pg. 131, September 1967.

25. J.P.Fidelle, L.R.Allemand, C.Roux and M.Rapin, "High Pressure Hydrogen Permeability of Metals at Room and Medium Temperatures", Colloquium Hydrogen in Metals, Valduc, edited by Le Centre d'Etudes de Bruyeres-le-Chatel, 91, France, pg. 209, September 1967.

26. T.E.Madey, "Adsorption and Displacement Processes on W 111 Involving CH_4, H_2, and O_2", Surface Science, Vol.29,pp.571-589, 1972.

27. D.L.Adams, L.H.Germer and J.W.Hay, "The Adsorption of Hydrogen on Tungsten (112), Coadsorption of Hydrogen with Oxygen", Surface Science, Vol.22, pp.173-178, 1970.

28. R.H.Cavett and H.C.Van Ness, "Embrittlement of Steel by High-Pressure Hydrogen Gas", Welding Journal, Welding Research Supplement, Vol. 42, pp. 316-319, July 1963.

29. G.G.Hancock and H.H.Johnson, "Hydrogen, Oxygen and Subcritical Crack Growth in a High Strength Steel", Transactions, American Institute of Mining, Metallurgical and Petroleum Engineers, Vol.236, No.4, pp.513-516, April 1966.

30. E. Fricke, H.P.Stuwe, and G.Vibrans, "Dissolution of Hydrogen From Gas in Steel", Met. Trans., Vol.2, No.9,pg.2697, Sep.1971.

31. P. Bastien and P. Azou, "Influence de l'Amplitude de la Vitesse des Deformations Plastiques sur las Segregation de l'Hydrogene dans le Fer et les Auers", Comptes Rendus, Vol.232,pg.69,1951.

32 J.A.Peterson, R.Gibala, and A.R.Troiano, "Hydrogen Induced Embrittlement and Internal Friction in Stable Austenitic Steel", Congress Hydrogen in Metals, Valduc Colloquium, pg. 200, 1967.

33. International Congress Hydrogen in Metals, Vol.1, Paris, pp.90-103, 1972.

34. R.M.Latanision and R.W.Staehle,"The Effect of Continuous Hydrogenation on the Deformation of Nickel Single Crystals", Scripta Metallurgica , Vol.2, pg. 667, 1968.

TABLES AND FIGURES

Composition	Inconel 718	L-605	A-286
	Heat 5595E	Heat L-1842	Heat 21 467
Fe	16.74	1.98	Bal.
Ni	54.02	9.60	24.86
Co		Bal.	
Cr	18.54	20.37	15.22
W		14.49	
Mo	3.2		1.24
Al	0.68		0.23
Ti	0.76		2.12
Mn	0.33	1.34	1.10
C	0.05	0.09	0.057
Si	0.31	0.65	0.60
Cb + Ta	5.28		
P		0.009	0.018
S	0.007	0.010	0.007
B			0.0015
V			0.33

Compositions

TABLE I

Material and Heat Treatment	Amount of Cold Work	Yield Strength Ksi		Tensile Strength Ksi		% Elongation		Superficial Hardness 15 N Scale
		L	T	L	T	L	T	
Inconel 718	35%	175	186	202	195	3	4	81
1800°F/1H + CR	20%	148	143	171	173	10	14	78.5
	0%	89		148		32		70
1725°F/1H 1325/8H FC. to 1150°F/8H		186		207		16		82.5
L - 605 2250°F/1H +CR	45%	242	230	264	275	2	4	84.5
A - 286 1800°F/1H +CR	50%	128	140	147	160	33	3.2	76
1800°F/1H 1325°F/ 16 H		115		155		20		76

Room Temperature - Mechanical Properties

TABLE II

P	1.6×10^{-9} $\frac{cm^3}{cm^2\ sec}$
D	4.5×10^{-9} cm^2/sec
S	0.36 cm^3 D_2/cm^3 metal
Q_P	9,300 cal/at g

Inconel 35% CW

180°C

Deuterium Gas - Experimental Values of Hydrogen Permeation

TABLE 111

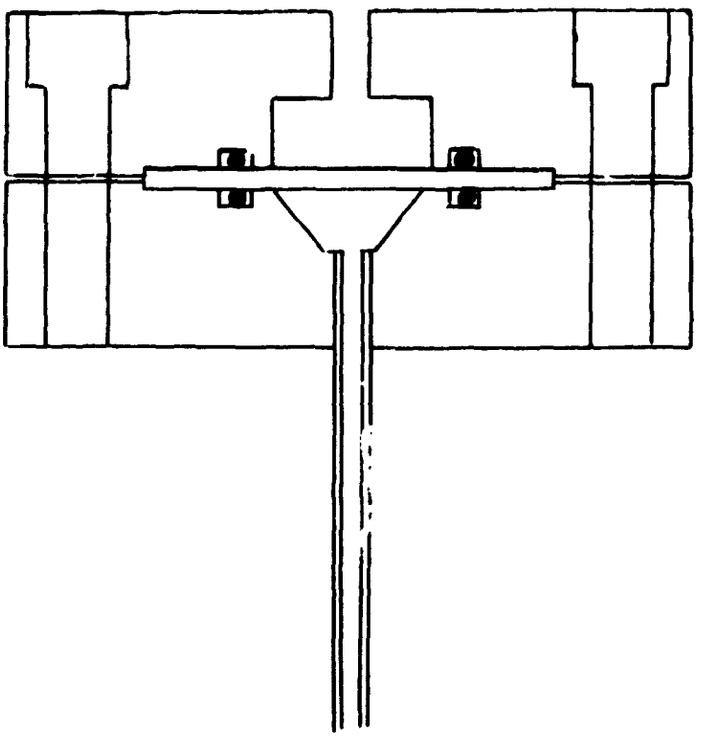

Disc Pressure Cell

Figure 1

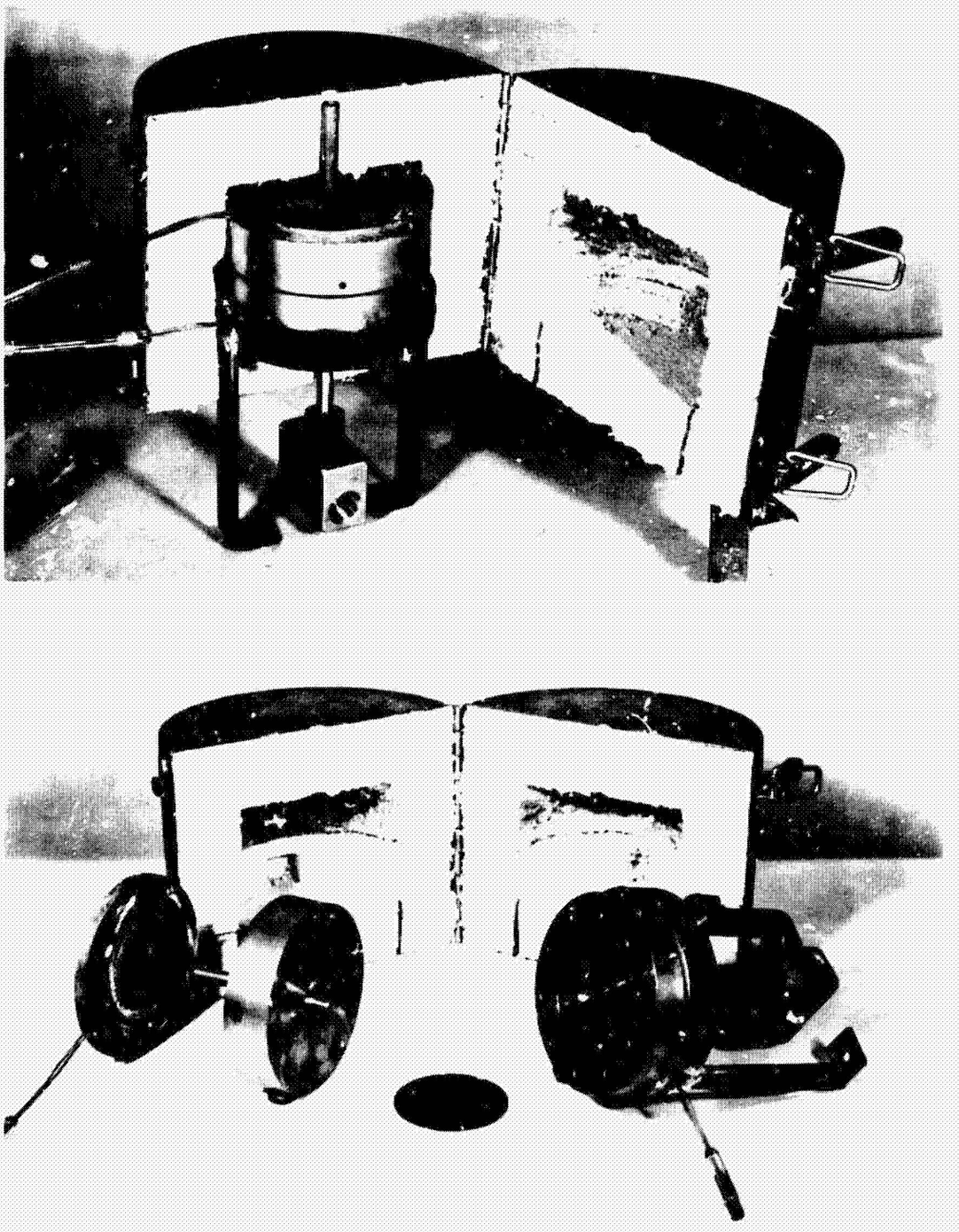

Figure 2 Disc Pressure Cell and Furnace Assembly

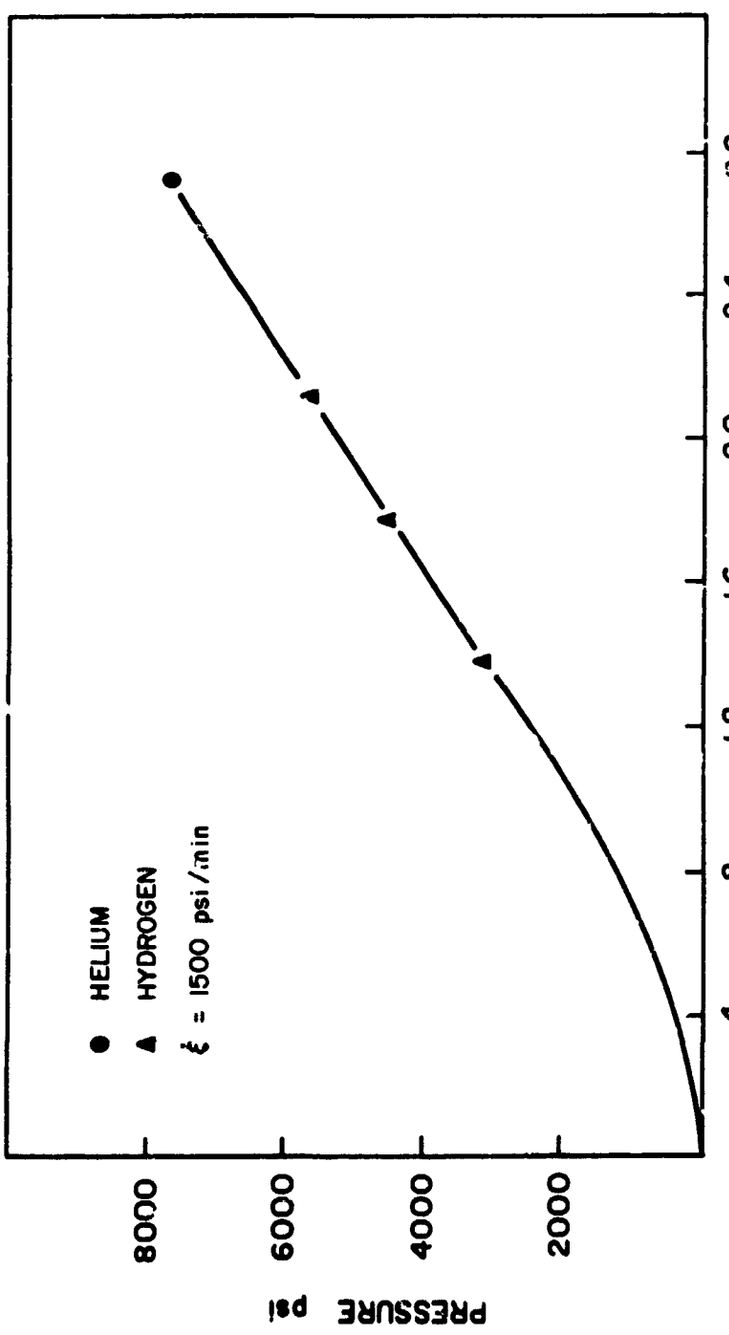

Figure 3 : Inconel 718 35% CW. Pressure vs. Deflection at Ambient Temperature

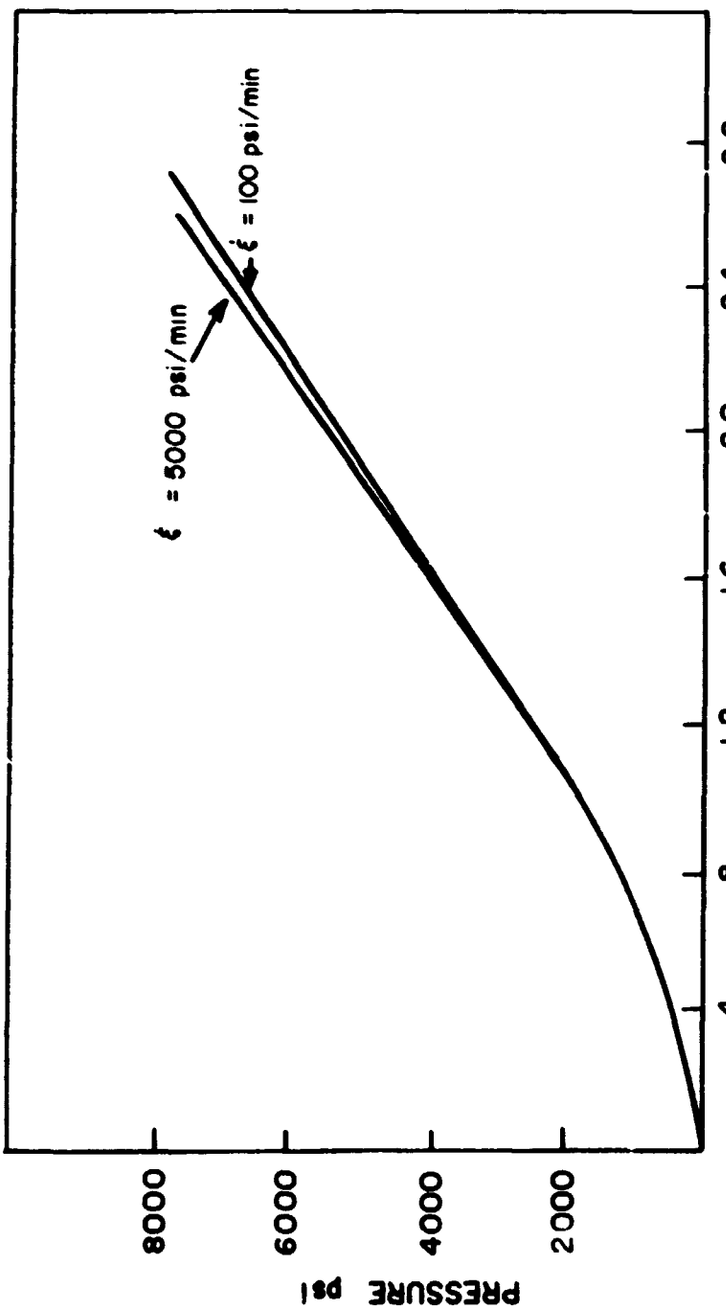

Figure 4 : Inconel 718 35% CW. Pressure vs. Deflection at Ambient Temperature in Helium

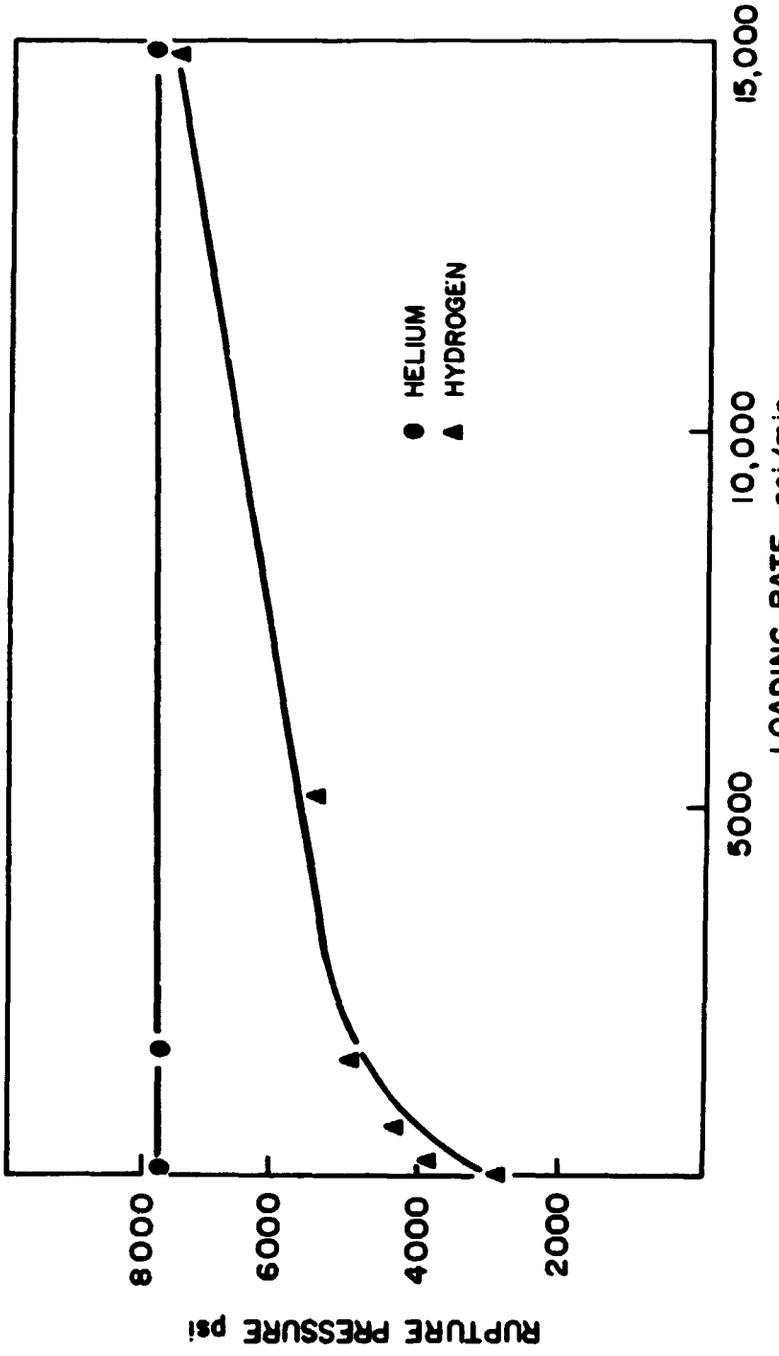

Figure 5 : Inconel 718 35% CW. Rupture Pressure vs. Loading Rate at Ambient Temperature

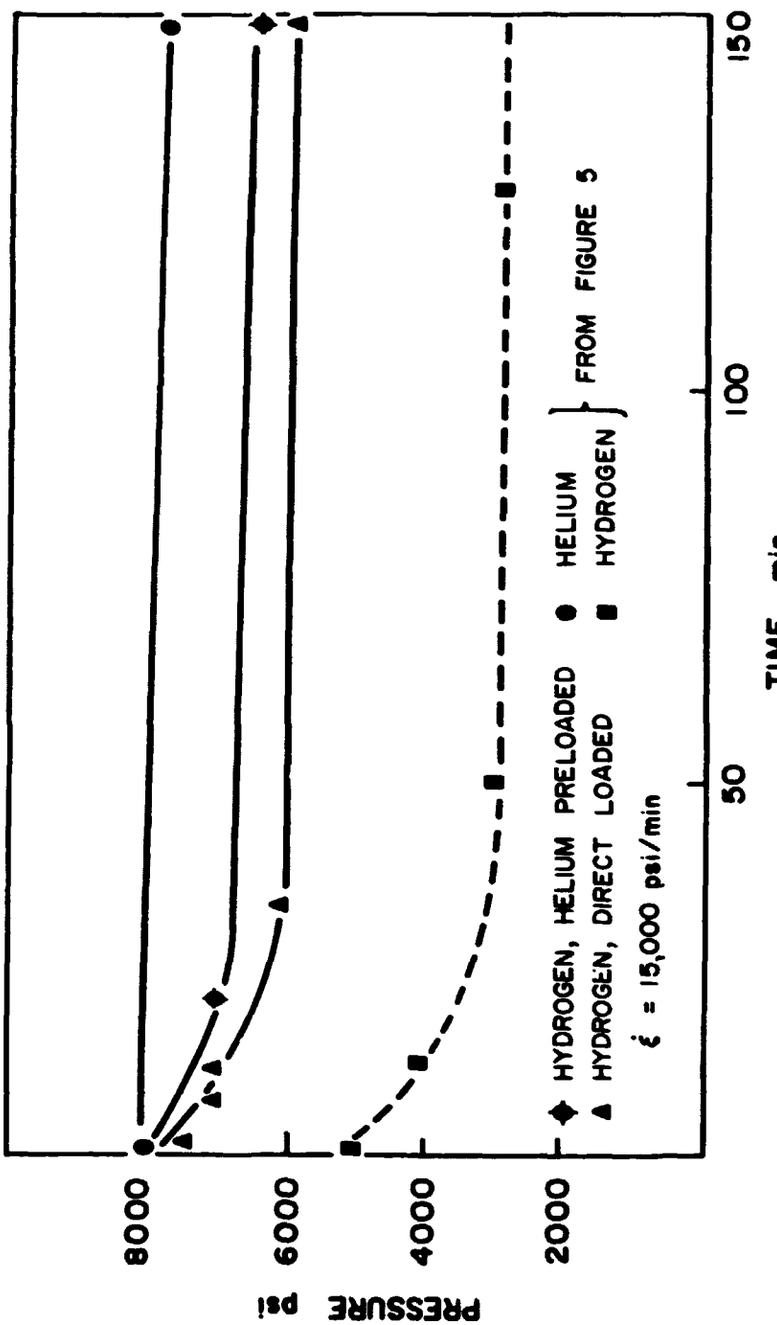

Figure 6 : Inconel 718 35% CW. Comparison of Hydrogen Delayed Failure at Ambient Temperature with and without Helium Preload

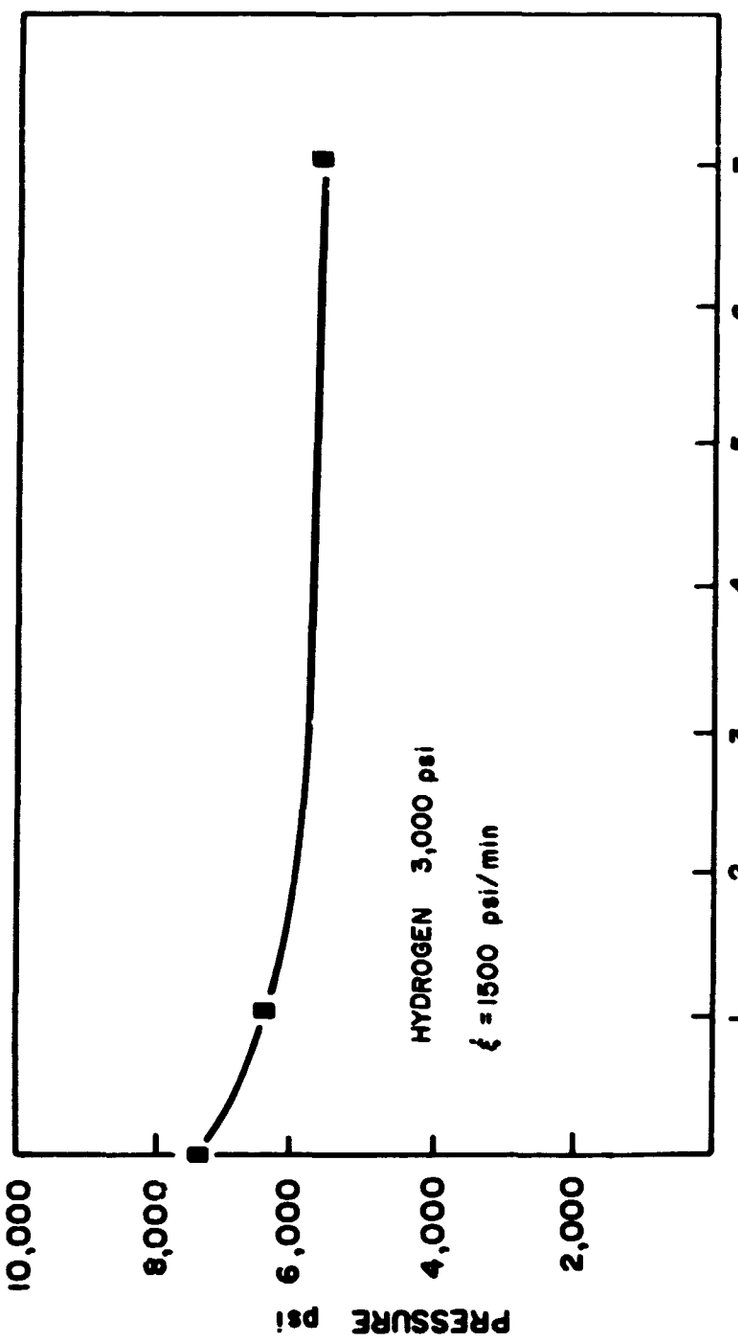

Figure 7 : Inconel 718 35% CW. Ambient Temperature. Rupture Pressure in Helium vs. Exposure Time in 3000 psi Hydrogen

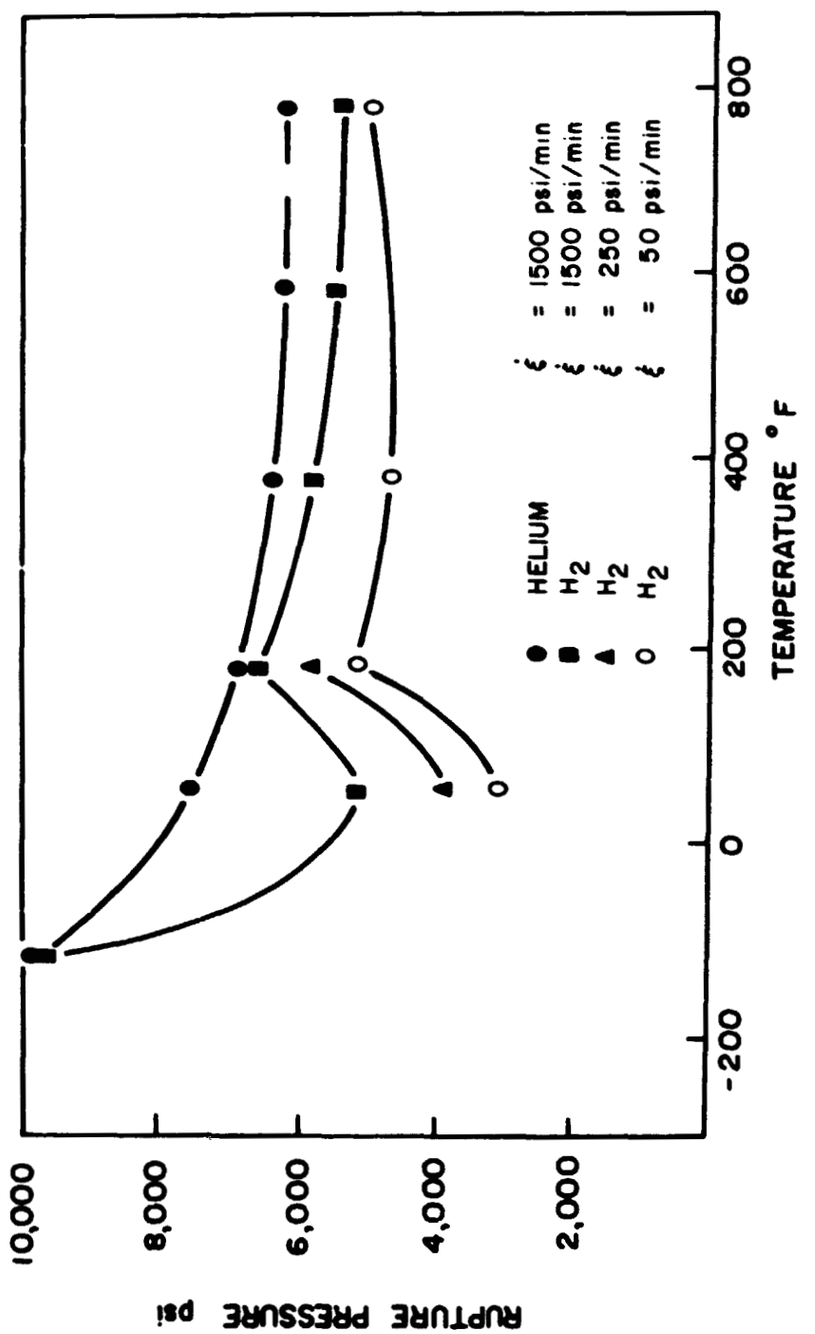

Figure 8 : Inconel 718 35% CW. Rupture Pressure vs. Temperature under Dynamic Loading

Procedure	Cyclic exposure Gas	Temperature RT - 800°F		Pressure 0 - 1000 psi		Final Rupture 1500 - psi/min		
		No. of Cycles	time/ cycle	No. of Cycles	time/ cycle	T(°F)	P(psi)	Gas
I (Fig.8)	He	1	1 hr.	0	0	800°	6250	He
II	He	1	100 hrs.	1	100 hrs.	800	5900	He
III (Fig.8)	H_2	1	1 hr.	0	0	800	5400	H_2
IV	H_2	1	100 hrs.	1	100 hrs.	800	5400	He
V	H_2	12	8 hrs.	1	100 hrs.	800	5400	He
VI	H_2	1	100 hrs.	50	4 min.	800	5400	He

Inconel 718, 35% CW

Cycling Procedures

Figure 9

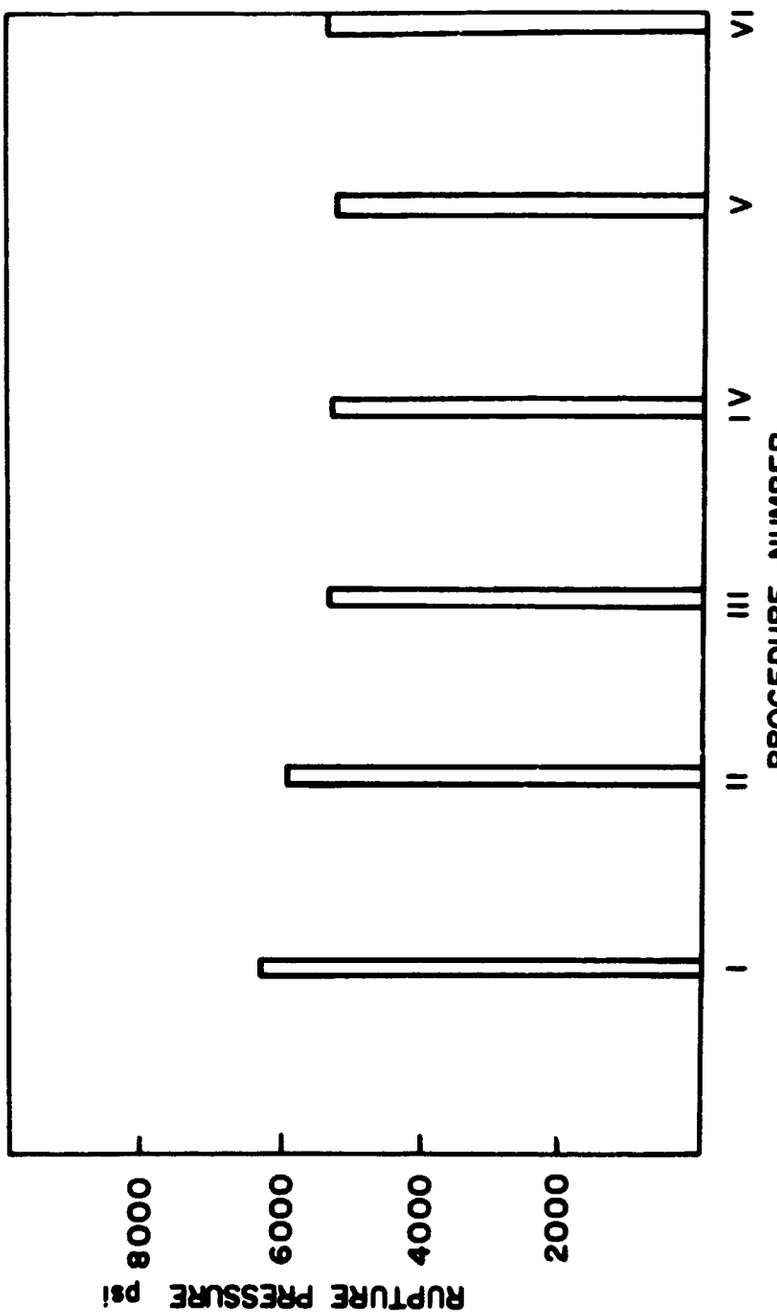

Figure 10 : Inconel 718 35% CW. Summary of Various Fatigue Testing Procedures

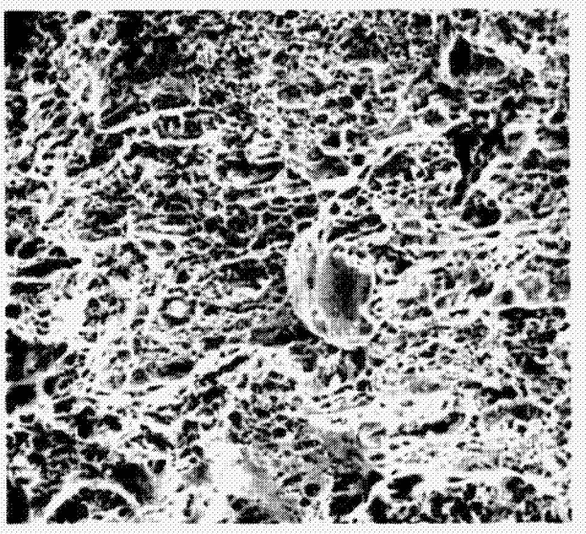

(a) Rupture in Helium 500X

Side in contact with Hydrogen

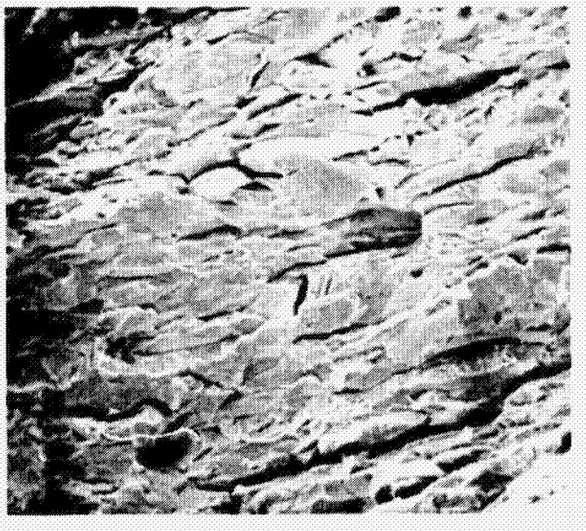

(b) Rupture in Hydrogen 500X

Figure 11 : Scanning electron micrographs of Inconel 718 (35% CW)

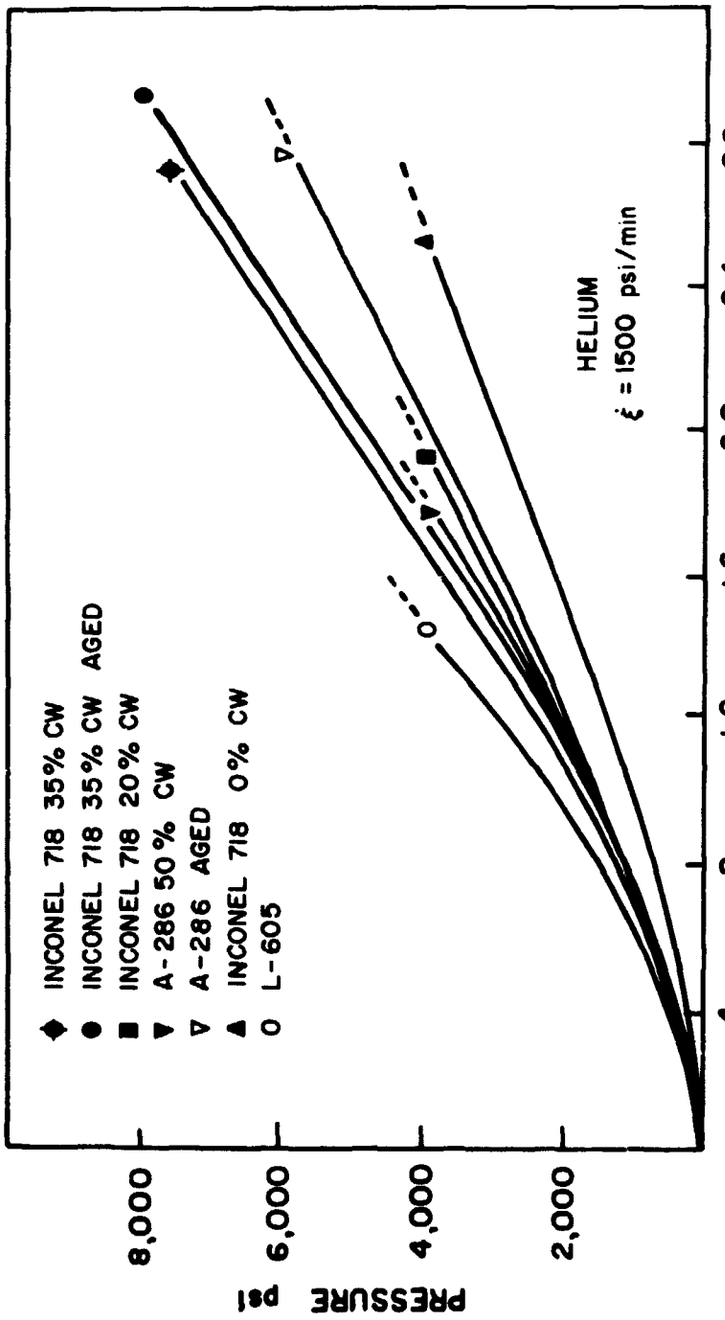

Figure 12 : Pressure vs. Deflection in Helium for All Alloys Examined

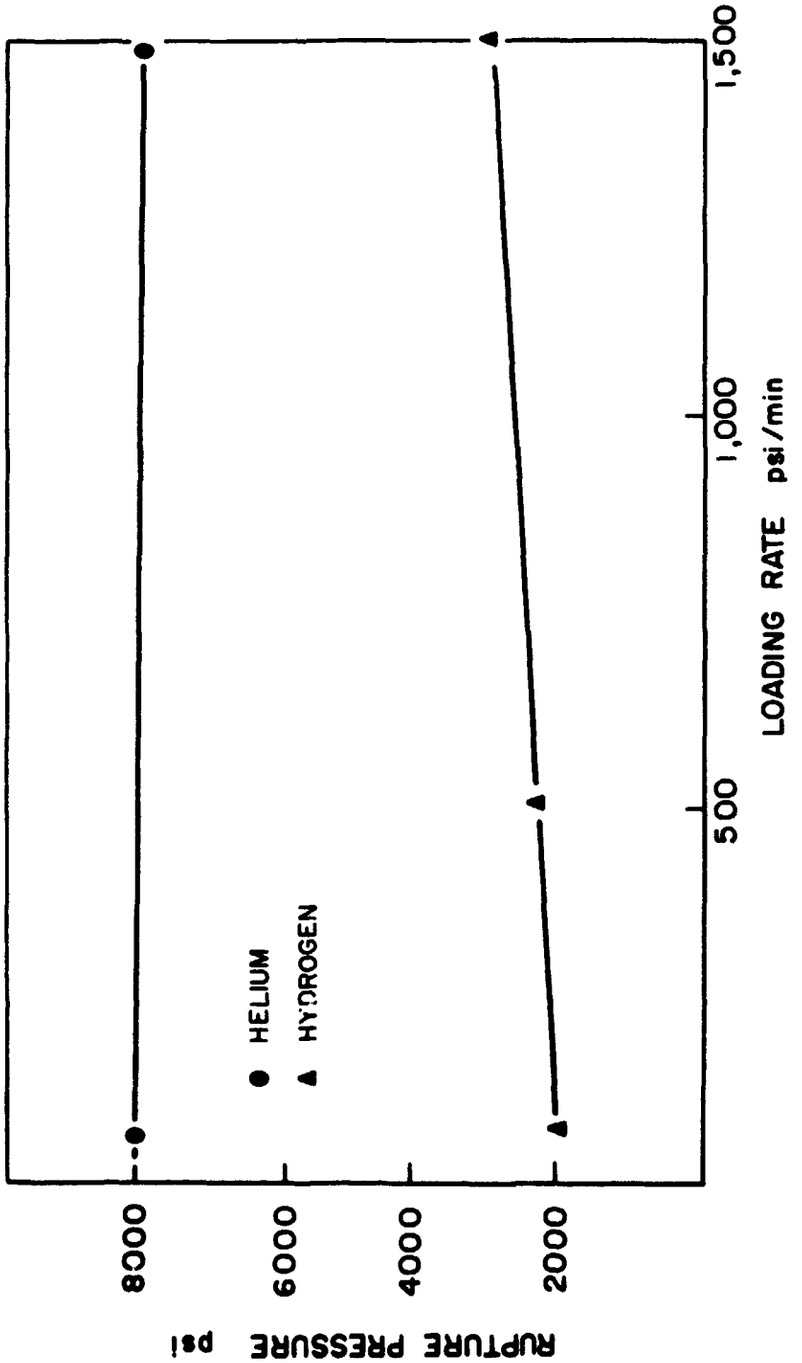

Figure 13 : Inconel 718 35% CW and Aged. Rupture Pressure vs. Loading Rate

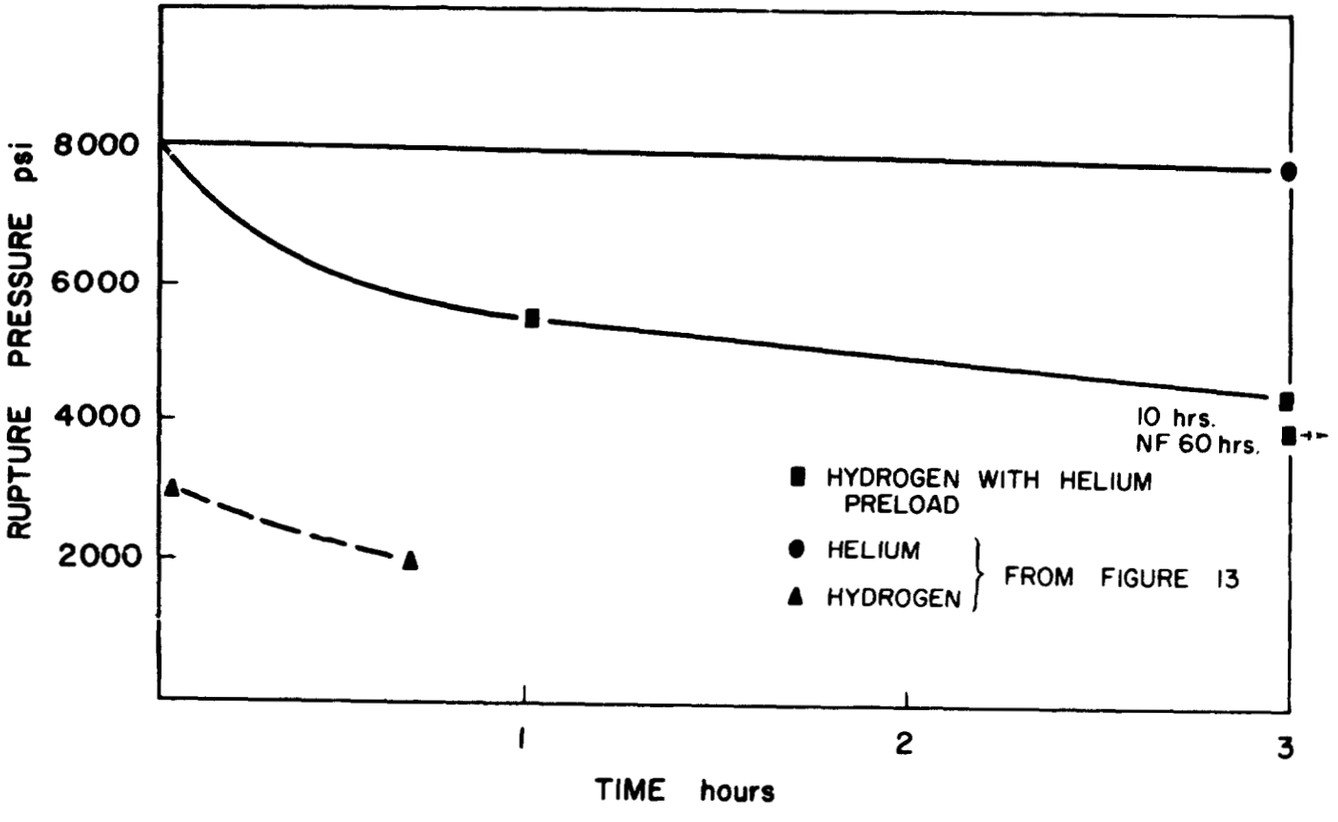

Figure 14 : Inconel 718 35% CW and Aged. Comparison of Hydrogen Delayed Failure at Ambient Temperature with and without Helium Preload.

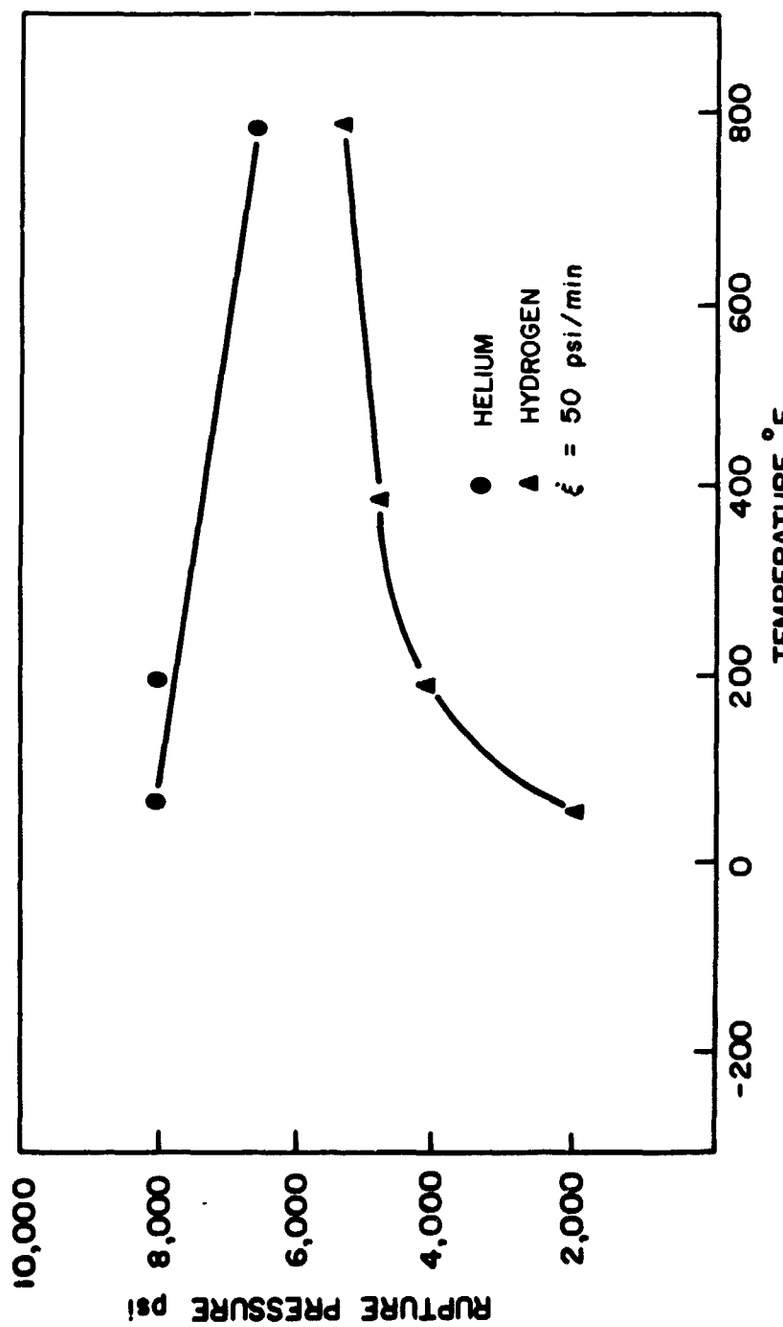

Figure 15 : Inconel 718 35% CW and Aged. Rupture Pressure vs. Temperature under Dynamic Loading

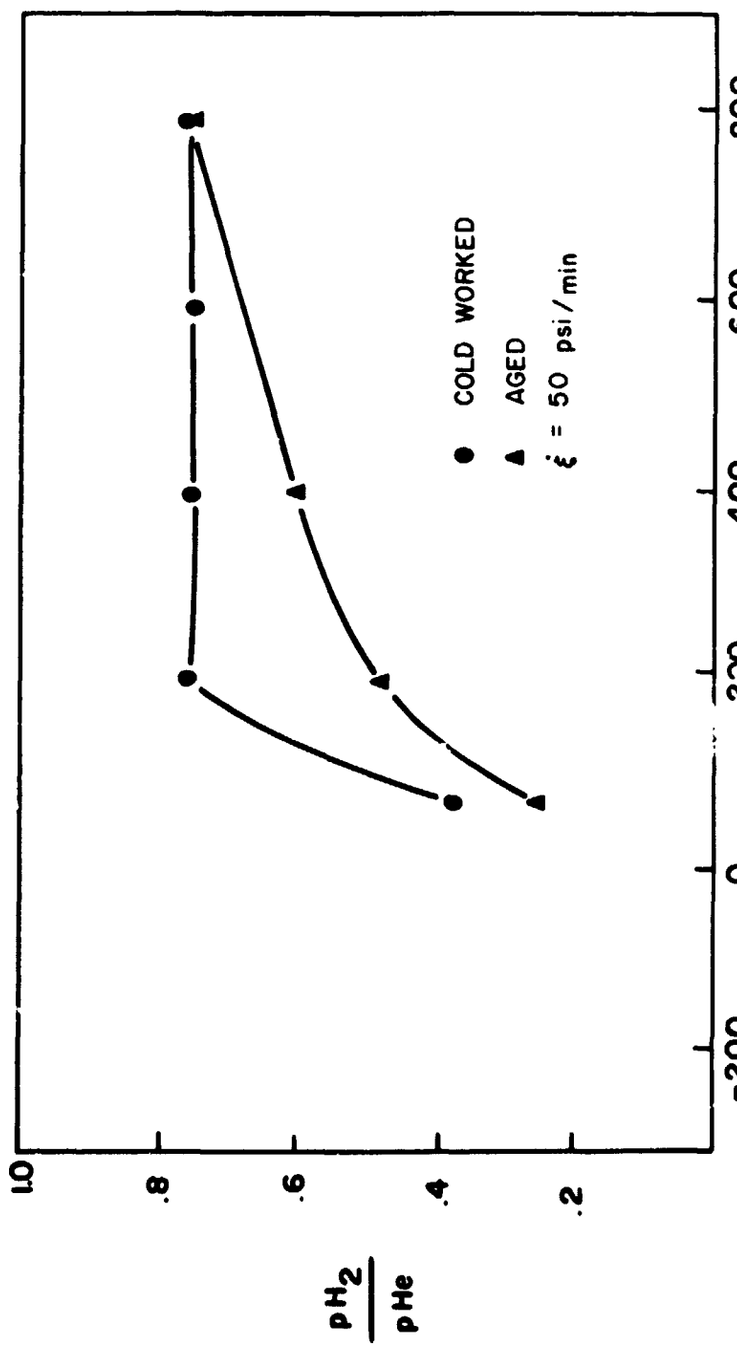

Figure 16 : Inconel 718 Ratio of Hydrogen to Helium Rupture Pressure vs. Temperature under Dynamic Loading

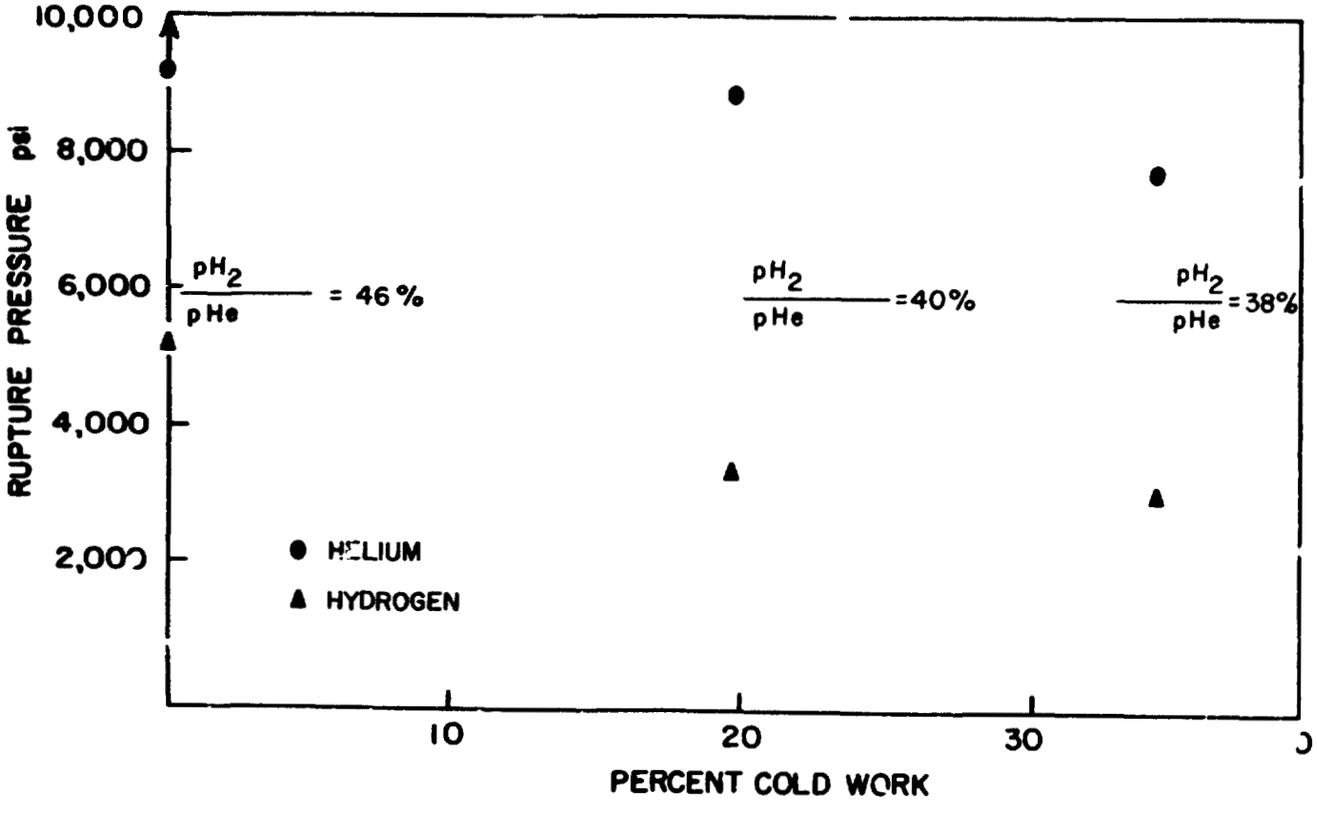

Figure 17 : Inconel 718 Influence of CW on Lowest Rupture Pressure under Dynamic Loading at Ambient Temperature

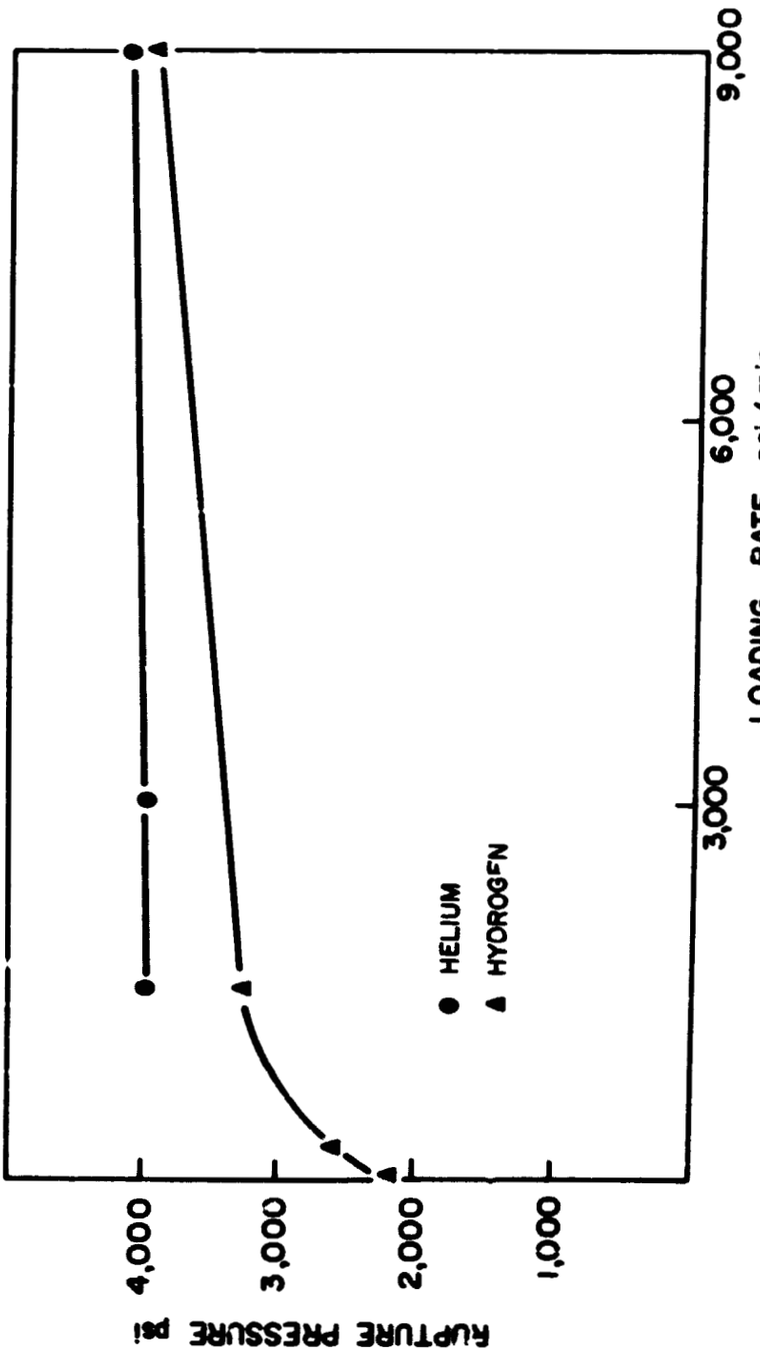

Figure 18 : L - 605 45% CW. Rupture Pressure vs. Loading Rate at Ambient Temperature

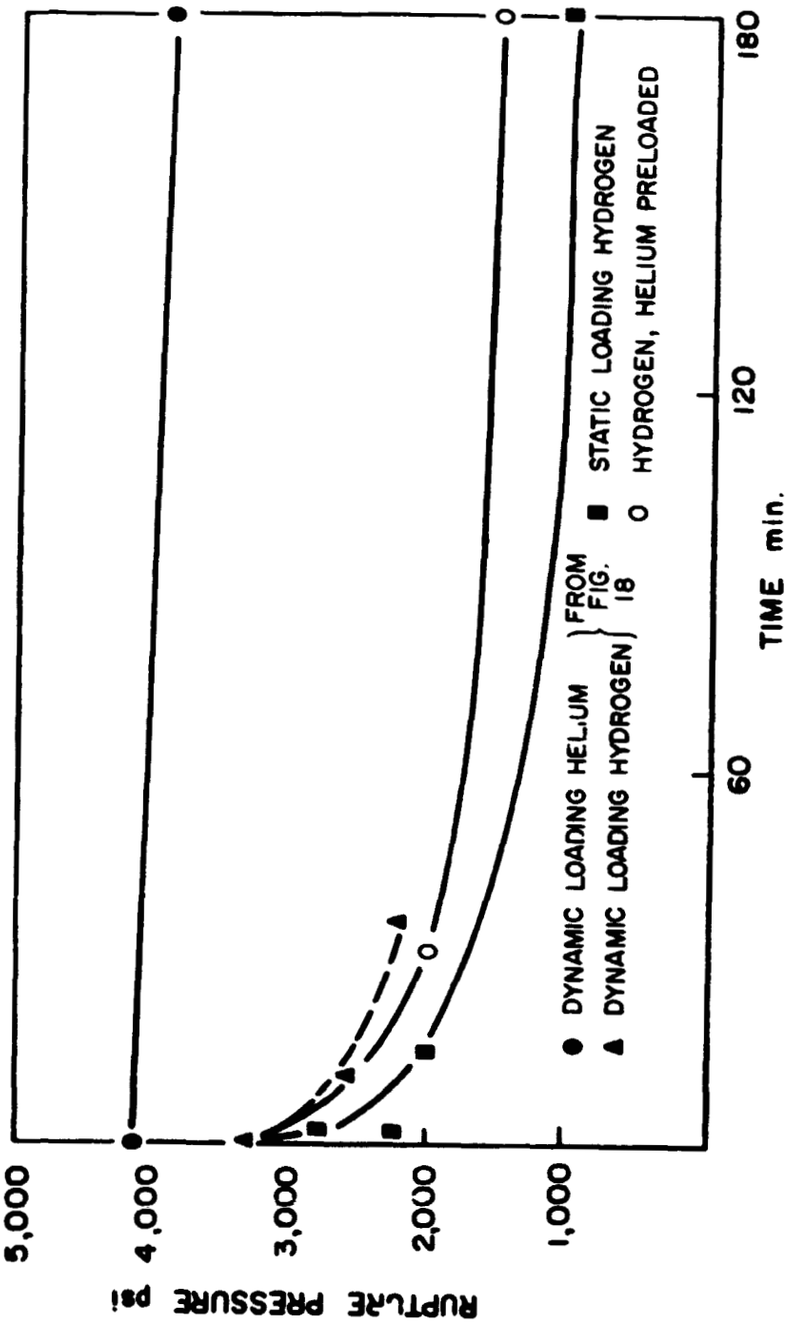

Figure 19 : L-605 45% CW. Rupture Pressure vs. Failure Time

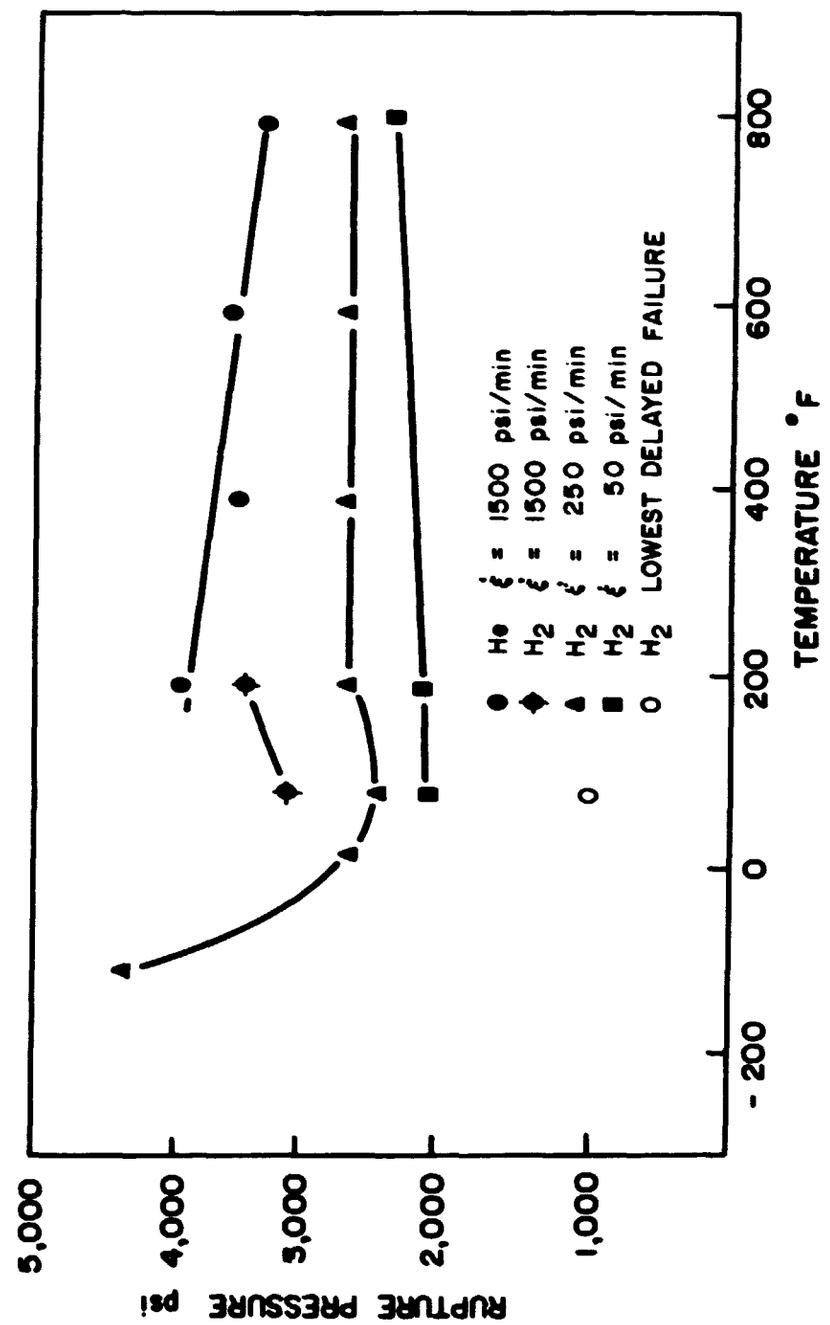

Figure 20 : L-605 45% CW. Rupture Pressure vs. Temperature under Dynamic Loading

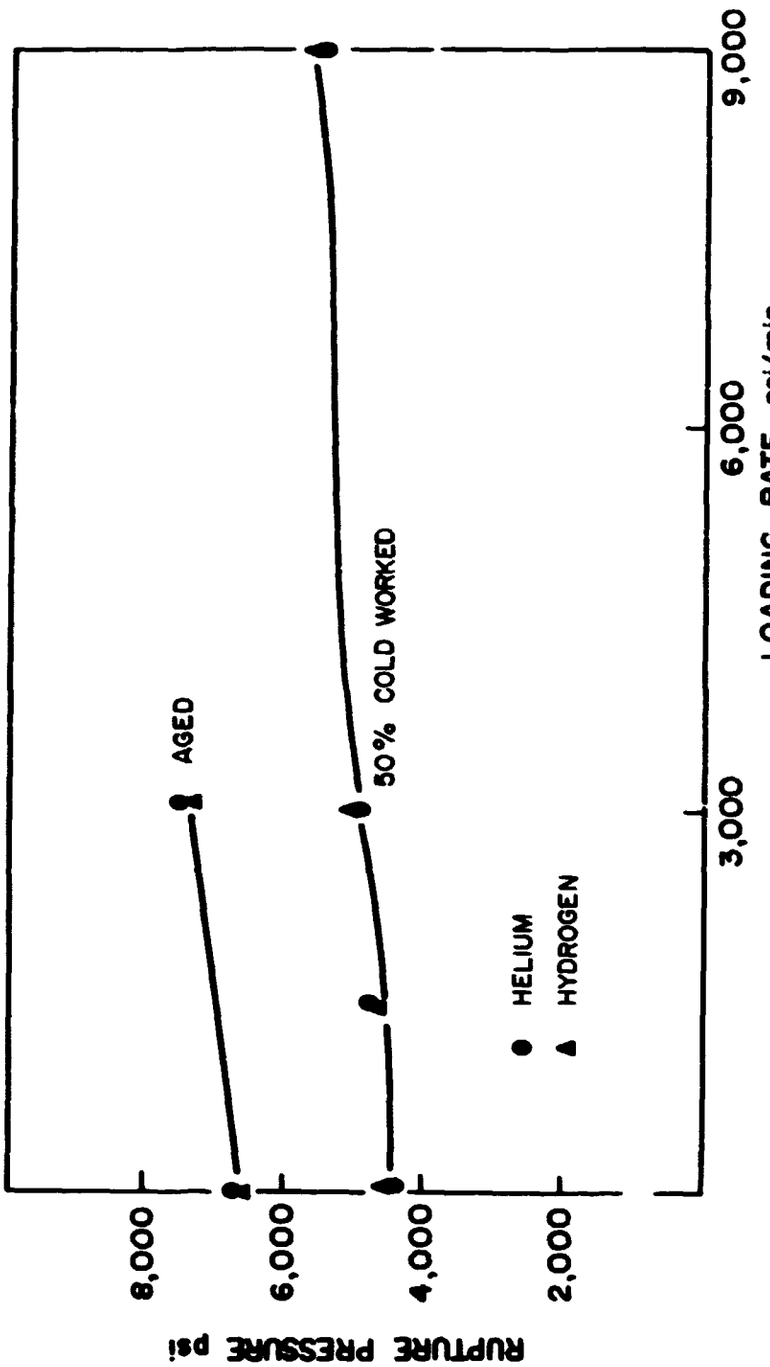

Figure 21 : A-286 Rupture Pressure vs. Loading Rate at Ambient Temperature

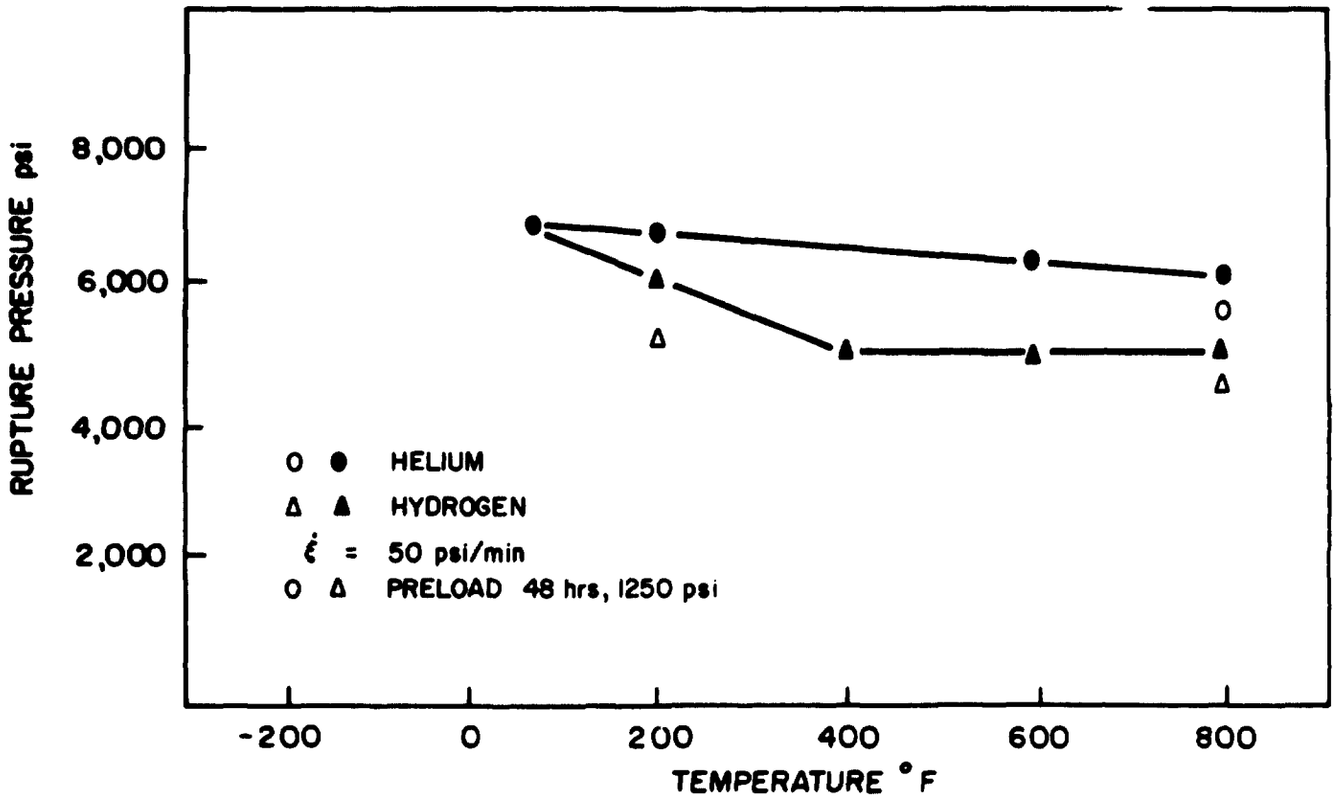

Figure 22 : A-286 Aged Rupture Pressure vs. Temperature under Dynamic Loading

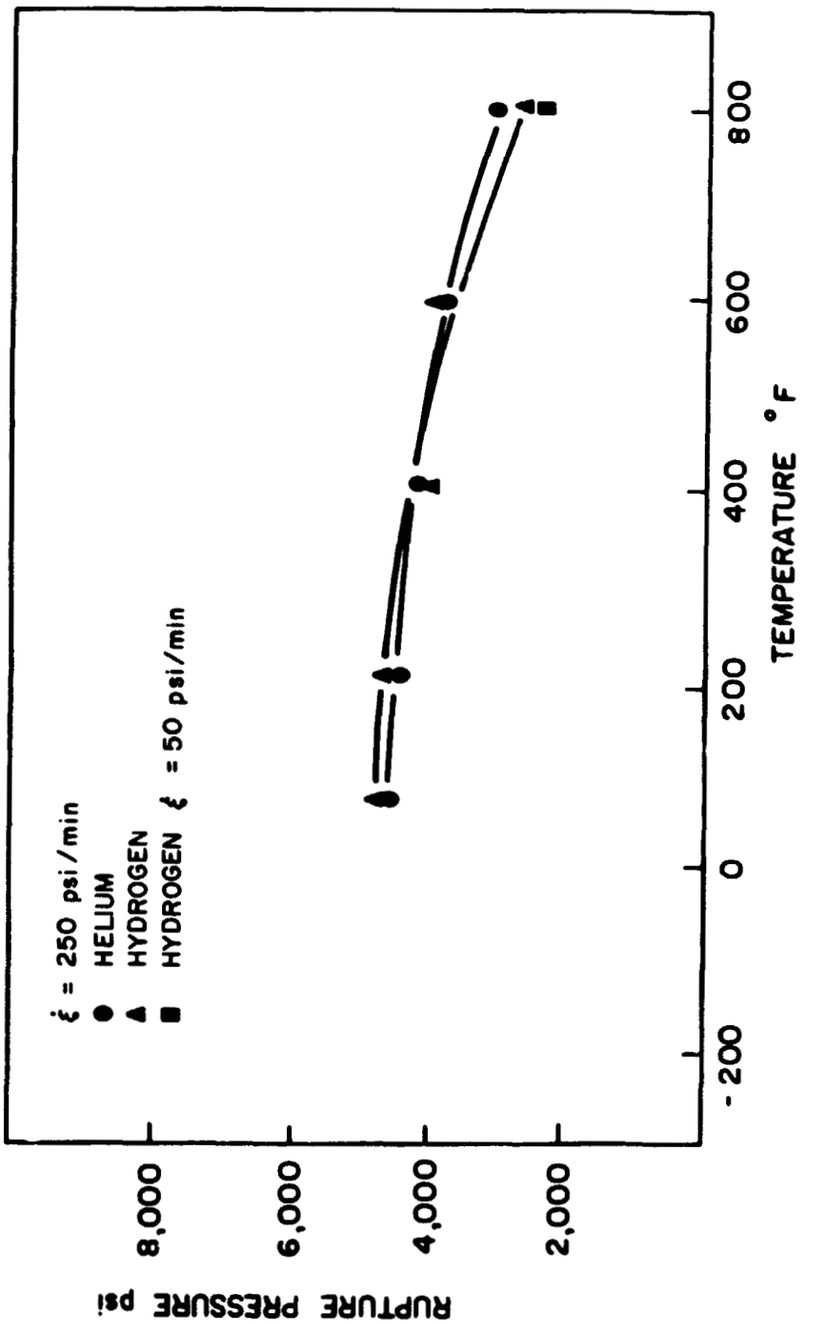

Figure 23 : A-286 50% CW. Rupture Pressure vs. Temperature under Dynamic Loading